Imaging Life

The Magazine for Molecular Imaging Innovation

SPECT•CT: Clinical Case Studies From Around the Globe
Special Edition | October 2012

SIEMENS

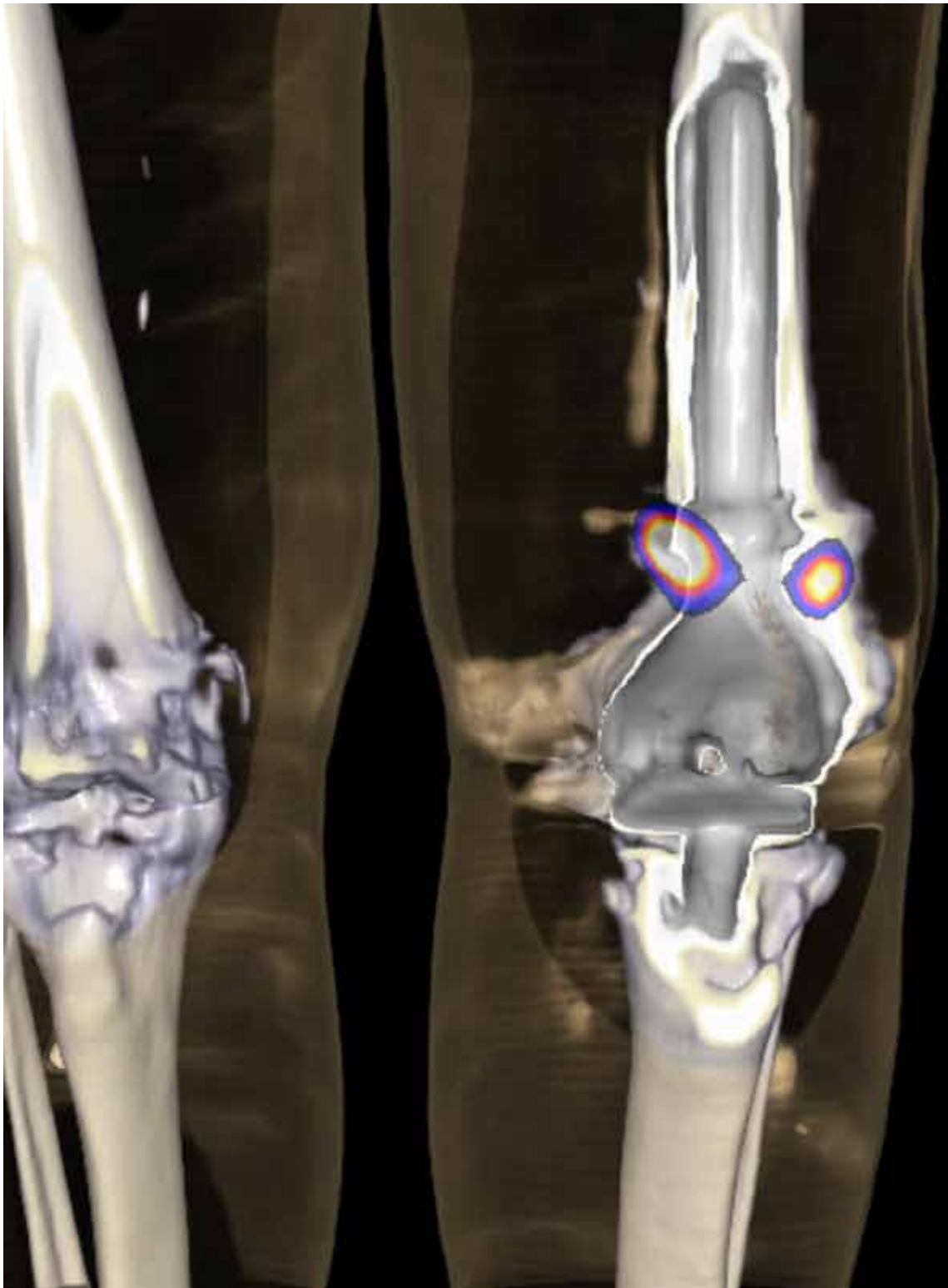

“Clinical cases involving high-demand Siemens Symbia SPECT•CT solutions derived from our worldwide clinical customer base.”

Alexander R. Zimmermann, Vice President
Marketing and Sales, Molecular Imaging, Siemens Healthcare

Cover page: Image was generated on Symbia™ T2 with low dose CT.

Alexander R. Zimmermann
Vice President
Marketing and Sales
Molecular Imaging
Siemens Healthcare

Dear Reader,

This Special Edition of *Imaging Life* highlights the groundbreaking imaging studies our global customers are performing with Siemens Symbia™ solutions to advance their lead in improving healthcare.

One of the most interesting developments in the growth of molecular imaging is the adoption of SPECT•CT. SPECT•CT combines functional information from SPECT with the exquisite anatomical details of CT to improve localization and disease evaluation.

As use of this technology grows, the need to share new applications and emerging advancements – achieved with Siemens technologies – across the nuclear medicine user spectrum intensifies.

Siemens introduced *Imaging Life* to facilitate the exchange of information between our customers and clinical experts. With this Special Edition of *Imaging Life* – which focuses on clinical cases involving high-demand Siemens Symbia SPECT•CT solutions derived from our worldwide clinical customer base with special focus on recent publications or conference presentations – we are providing another tool to help our users discover new applications their colleagues have identified to aid in diagnosis and treatment decisions.

When you read through these Case Studies, keep in mind how you can use these SPECT•CT strategies – and the 2-, 6- or 16-slice Symbia T – to achieve new levels of success in your practice of surgical planning, orthopedics, advanced cardiology and more.

Enjoy reading,

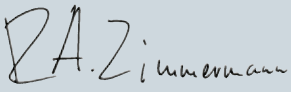

Alexander R. Zimmermann

Contents

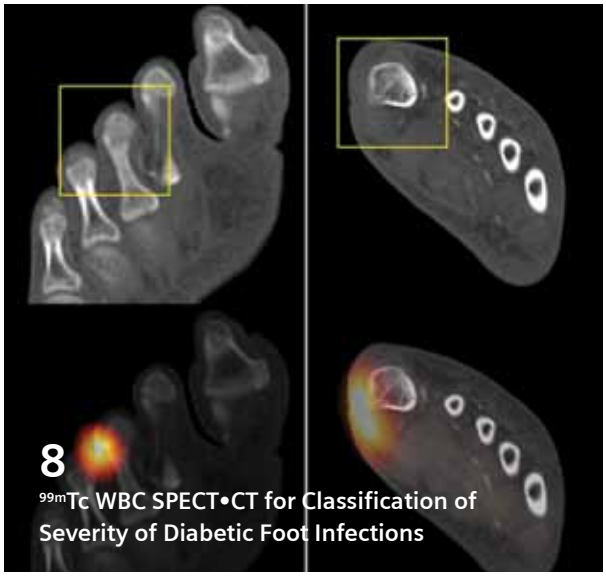

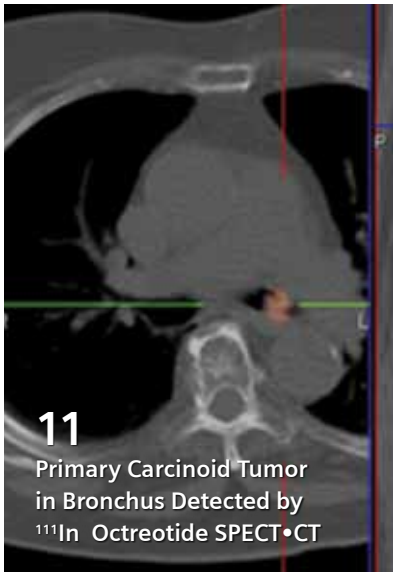

Imaging Life

Everything from the world of molecular imaging innovations. This semi-annual magazine presents clinical case reports and applications, customer experiences and product news and is primarily designed for physicians, hospital management and researchers.

For current or past issues, visit: siemens.com/imaginglife

Clinical Case Studies

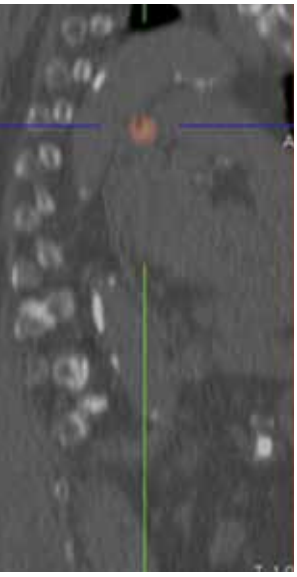

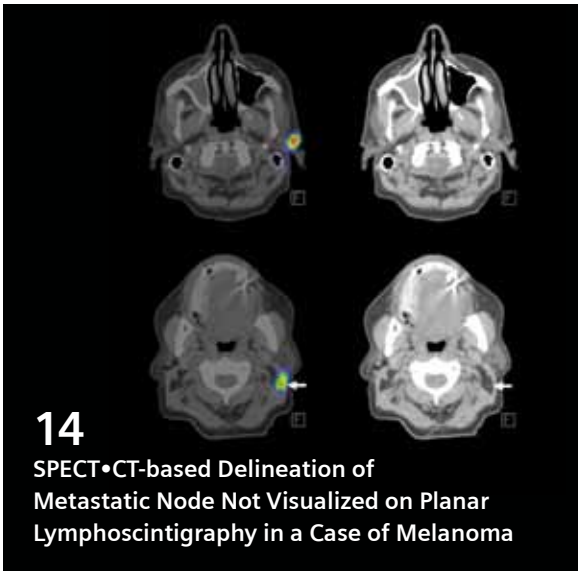

14
SPECT•CT-based Delineation of Metastatic Node Not Visualized on Planar Lymphoscintigraphy in a Case of Melanoma

22
Precise Localization of a 'Hot Screw' After Total Knee Replacement Demonstrated by SPECT•CT

Case 1
SPECT•CT Evaluation of Painful Knee Joint Following ACL Reconstruction

By Michael Hirschmann, MD and Helmut Rasch, MD

Case study data provided by the Department of Orthopedic Surgery, Kantosspital Baselland, Bruderholz, Switzerland

INTRODUCTION

Current therapy for injury to or tear of the Anterior Cruciate Ligament (ACL) is ACL reconstruction using muscle or tendon graft fixed with interference screws. Biodegradable interference screws offer fixation strength, while requiring no screw removal. However, complications such as delayed degradation, screw breakage and foreign body reaction have been reported and may cause severe knee joint movement limitation and pain. SPECT•CT imaging of skeletal metabolism with integrated diagnostic CT offers a comprehensive evaluation due to a combination of morphological and functional information essential for accurate assessment of the joint and graft biology. This case study demonstrates the value of SPECT•CT imaging in the delineation of foreign body reaction and delayed degradation of biodegradable interference screws, causing pain and limitation of movement in a patient following ACL reconstruction.

1

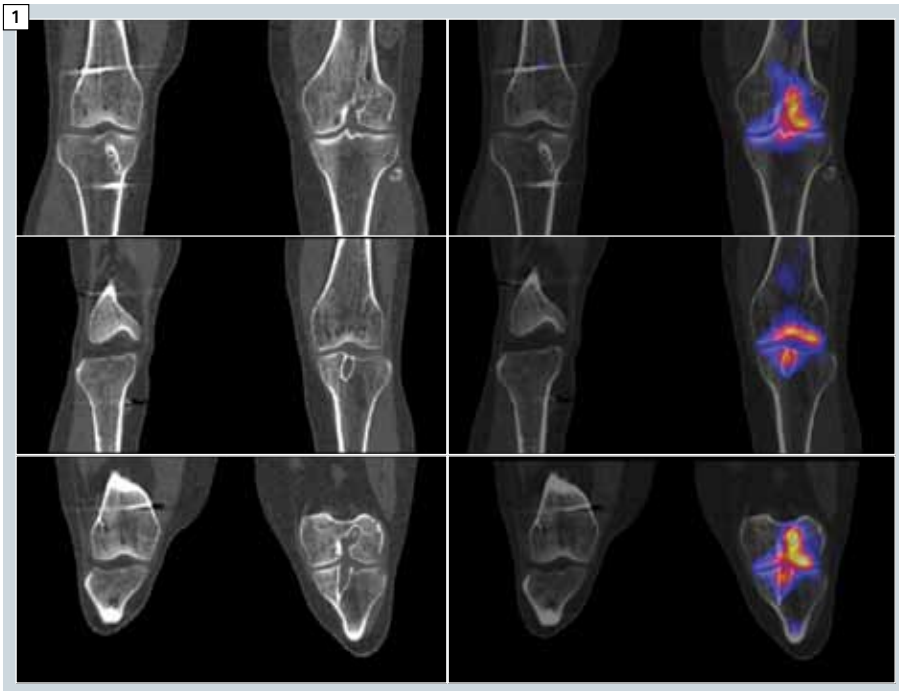

1 ^{99m}Tc MDP SPECT•CT coronal images show left femoral and tibial tunnels with diffuse patchy osteopenia in the adjacent bone, predominantly in the lower end of the femur seen on thin-slice CT. Increased tracer uptake is visualized within the tibial and femoral tunnels, as well as around the patellofemoral joint. The contralateral knee shows evidence of past surgery, with the tibial and femoral tunnels showing no tracer uptake.

HISTORY

A 29-year-old woman sustained a left knee injury during a skiing accident that was diagnosed as an ACL tear, along with a radial lesion of the lateral meniscus. The patient underwent arthroscopically assisted ACL reconstruction using a bone-patellar tendon-bone (BTB) autograft 3 months after the injury. A tibial and femoral tunnel was created for the placement of the autograft, and the graft was fixed with biodegradable interference screws. In addition, a partial lateral meniscectomy was performed.
The patient had undergone a similar surgery in the contralateral knee 8 years before using patellar tendon autograft, without complications.
Six months following the left knee ACL reconstruction, the patient was evaluated again for continued pain and limited flexion of the knee joint. Climbing stairs caused excruciating knee pain, along with lack of knee stability. Patient underwent a technetium-99m methylenediphosphonate (^{99m}Tc MDP) SPECT•CT study on a Symbia™ T scanner. The patient underwent revision arthroscopy, which showed diffuse hypertrophy of synovium, as well as a cyclops lesion of the ACL graft that caused graft to notch roof impingement in extension. The interference screws were partially degraded.

DIAGNOSIS

The interference screws were removed and debridement of the ACL graft with arthrolysis of the anterior patellar ligament interval was performed.

2

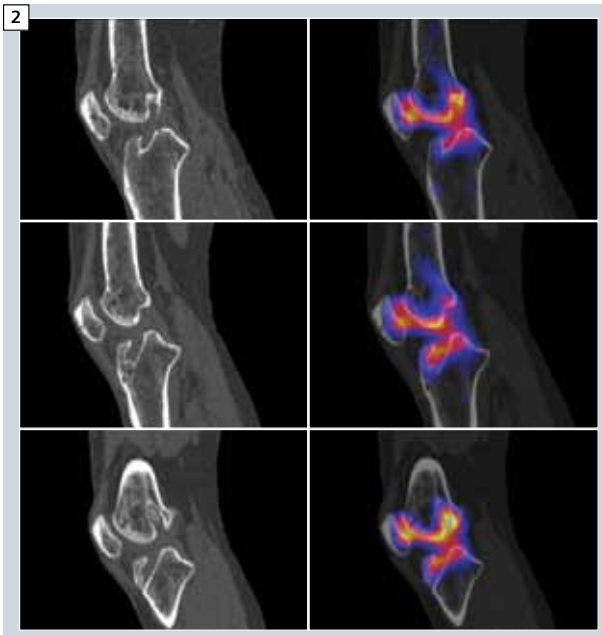

2 Sagittal CT and SPECT•CT fused images show tibial and femoral tunnels with corresponding increased uptake that extends to the patellofemoral space. Remnants of tendon graft are visualized within the tunnels on CT.

3

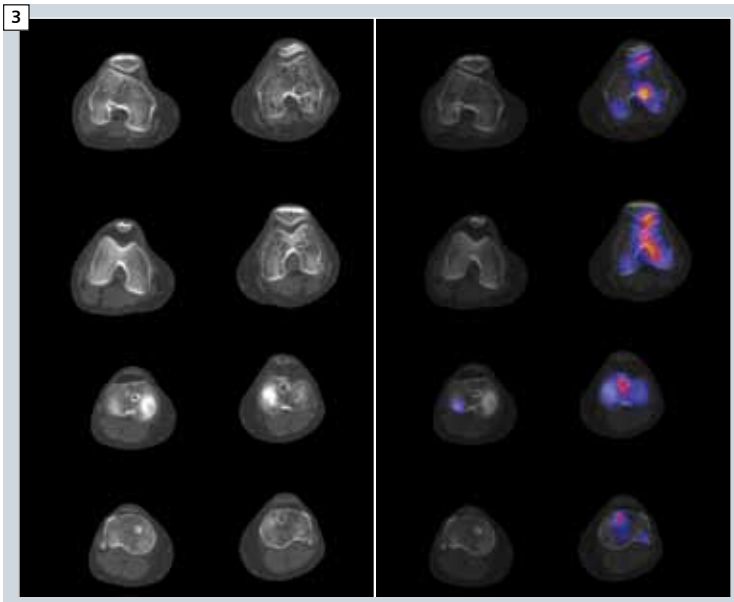

3 Axial images show the regions of increased uptake, as well as the larger tibial and femoral tunnel diameter in the left knee compared to that in the contralateral knee.

Histological examination of the degraded screw material and removed fibrous tissue showed typical findings of foreign body reaction. The patient fully recovered from surgery, was pain-free in the left knee and regained full mobility of the joint.

The pain and limitation of movement in the left knee was related to a combination of improper graft placement, delayed degradation of the biodegradable interference screws and subsequent foreign body reaction to the screws.

4

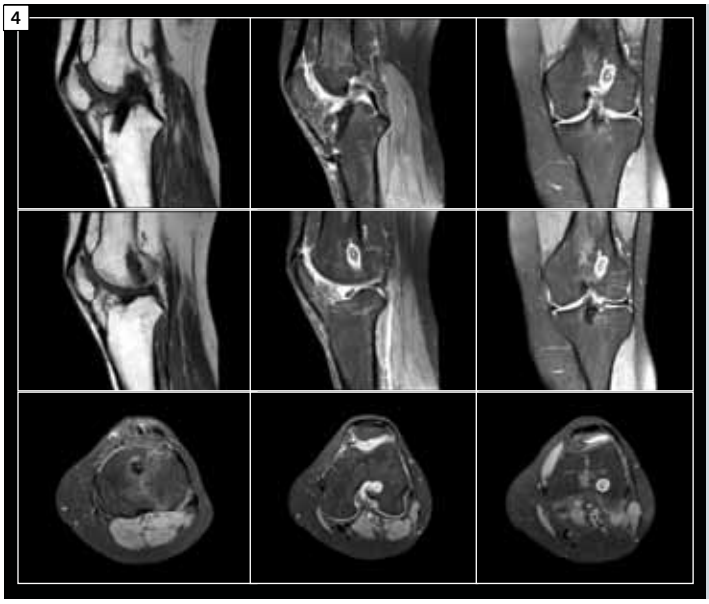

4 An MRI performed following SPECT•CT demonstrated intact ACL graft and a tibial cyclops lesion (fibrocartilagenous nodule in the anterior portion of the ACL graft), along with a patella infera (abnormally low patella). There was no fluid collection within the bone tunnels.

COMMENTS

Symbia T6 SPECT•CT provided information that led to the surgical decision to debride the ACL graft and remove the interference screws, as well as for the arthrolysis of the anterior patellar ligament interval. Symbia T CT technology offers the smallest focal spot size in its class and fine detector collimation of 6 x 0.5 mm.* Thin-slice CT demonstrated the widening of the femoral and tibial tunnel, as well as the increased metabolic activity within the tunnels secondary to graft remodeling and the patellofemoral joint due to the rod impingement during extension. This case highlights the value of Symbia SPECT•CT in the evaluation of joint pain.

EXAMINATION PROTOCOL

Scanner	*Symbia T6*
Dose	***20 mCi ^{99m}Tc MDP***
Parameters	***64 frames, 20 sec/frame***
CT	***130 kV, 60 mAs, 1 mm slices***

*Based on competitive information available at time of publication. Data on file.

Case 2

^{99m}Tc WBC SPECT•CT for Classification of Severity of Diabetic Foot Infections

By William Erdman, MD

Case study data provided by University of Texas Southwestern Medical Center, Dallas, Texas, USA

INTRODUCTION

Imaging of infection using radiolabeled white blood cells with SPECT or SPECT•CT shows high specificity. A combination of integrated diagnostic CT with SPECT using radiolabeled infection imaging agents can improve the localization and characterization of infective foci. Such an approach has been used in the evaluation of diabetic foot infections to differentiate between soft tissue infection and infections with osteomyelitis. A Composite Severity Index (CSI) was proposed to classify the severity of diabetic foot infection based on parameters obtained from SPECT•CT imaging, which includes intensity of technetium-99m white blood cell (^{99m}Tc WBC) uptake, degree of extension of ^{99m}Tc WBC into adjacent bone (presence of osteomyelitis and marrow invasion) and number of tracer avid lesions.

The system for staging of diabetic foot infection using SPECT•CT imaging with radiolabeled WBC is as follows:

- **Soft Tissue Infection (Stage 0)**
  Abnormal soft tissue WBC accumulation does not extend to the cortex of the bone
- **Osteomyelitis (Stage I/II/III)**
  Stage I: Abnormal WBC accumulation extends to the cortex of the bones, but does not cause cortical abnormality on CT
  Stage II: WBC accumulation associated with cortical erosion on CT
  Stage III: WBC accumulation with cortical erosion and extension into marrow on CT

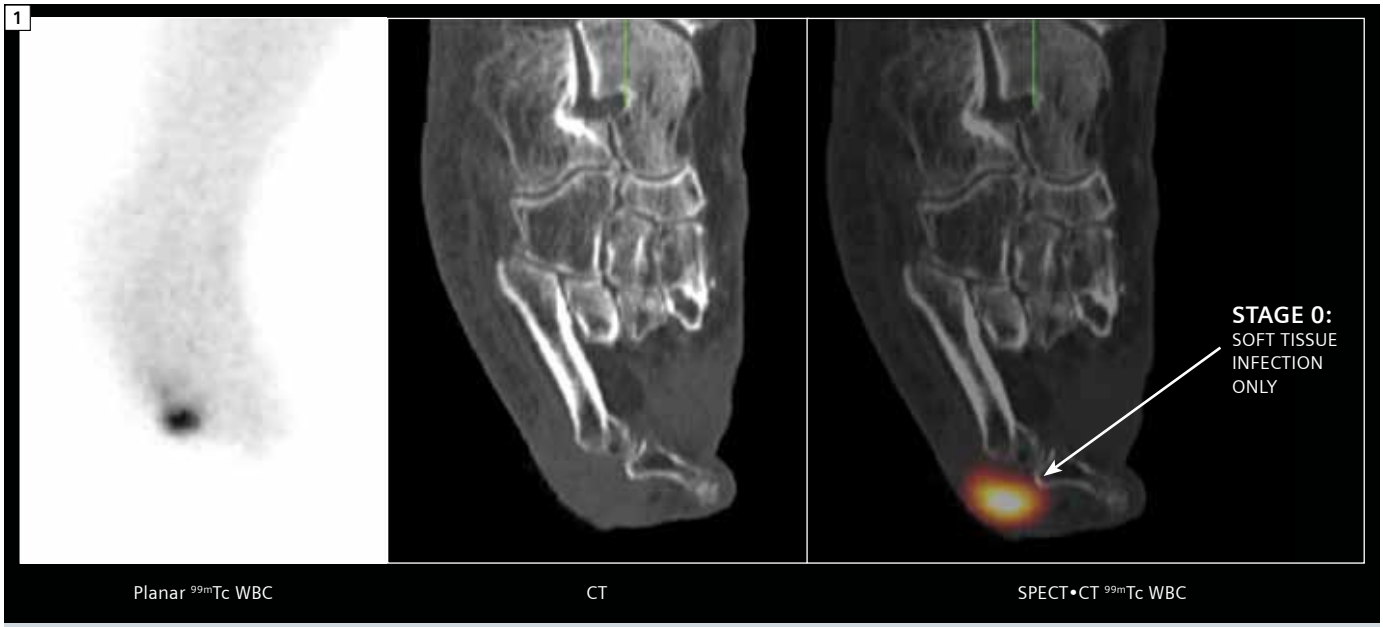

1 Planar, CT and SPECT•CT fused images of a patient with diabetic foot infection who underwent ^{99m}Tc WBC SPECT•CT. A planar scintigram shows intense focal increase in uptake, which was much higher than the background and blood vessel activity. Thin-slice diagnostic CT showed no erosion of the metatarsals and phalanges and the first metatarso-phalangeal joint. Fused images show the focal area of increased uptake of ^{99m}Tc WBC to be confined to the subcutaneous soft tissue adjacent to the bony margins, but separate from the bone without any infiltration. This study was classified to be soft tissue infection only (Stage 0).

DIAGNOSIS

To further facilitate SPECT•CT-based characterization of diabetic foot infection, each individual foci of infection was given an intensity score and stage score:

Intensity (^{99m}Tc WBC activity relative to blood vessels)

- **0** WBC activity below blood vessel activity
- **1** Focal WBC activity equal to blood vessel activity
- **2** Moderate focal increase above blood vessel activity
- **3** Intense focal increase above blood vessel activity

Stage (Relationship of WBC focus to bone cortex, cortical erosion and marrow involvement)

- **0** WBC activity limited within soft tissue; does not extend to the cortex of the bone
- **I** WBC activity extends to the cortex, but does not cause cortical erosion on CT
- **II** WBC activity extends to the cortex of the bone and causes cortical erosion on CT
- **III** WBC activity extends through the cortex of the bone and into the marrow space with erosion of cortical bone on CT

If there are two or more lesions in a foot then the intensity and stage scores are summed.

The CSI reflects the overall severity of infection in a foot based on multiplicity of lesions, stage and intensity of ^{99m}Tc WBC uptake.

CSI = (sum of lesion intensity scores [0–3]) + (sum of lesion stage scores [0–III]).

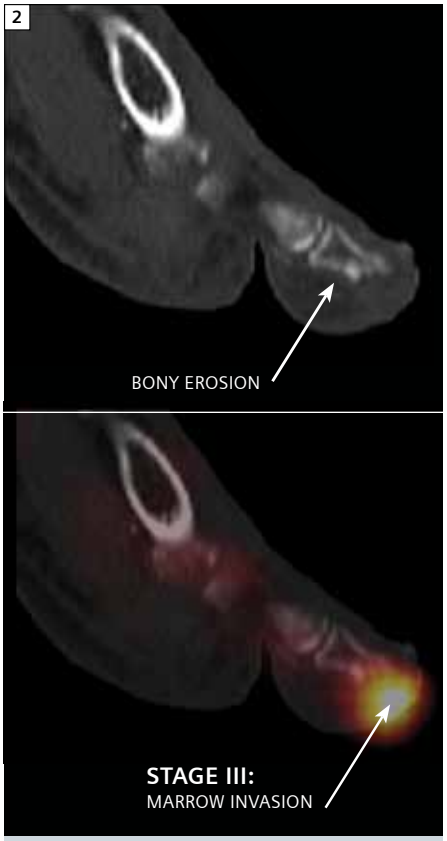

2 A ^{99m}Tc WBC SPECT•CT study of another patient with diabetic foot infection. CT shows bony erosion in the end of the distal phalanx of the big toe. SPECT•CT fused images show increased tracer uptake in the soft tissue encroaching into the bone corresponding to the region of bony erosion, which suggests the presence of osteomyelitis with marrow invasion of the infection process (Stage III).

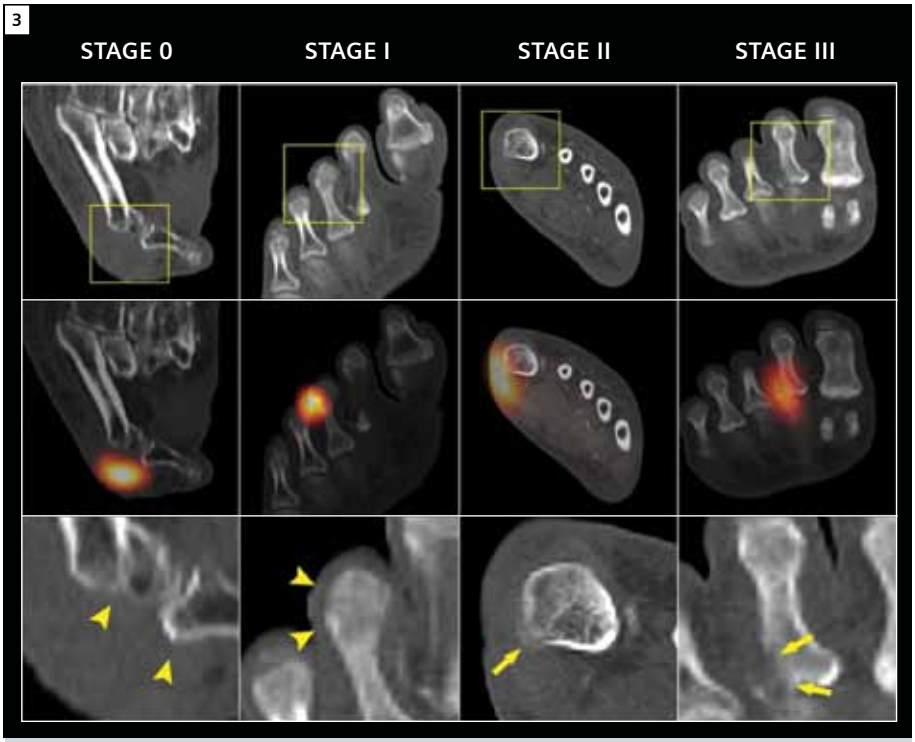

3 CT and SPECT•CT fused images following a ^{99m}Tc WBC injection of four different patients with diabetic foot infection with progressive stages of infection. Stage 0 shows only soft tissue infection. Stage I shows ^{99m}Tc WBC uptake extending to the bony margin (arrowheads), but without any erosion seen on CT. Stage II shows extension of the infective process and tracer uptake into the cortex with CT changes, including periosteal reaction and slight cortical erosion. Stage III shows infiltration of infective process into the bone with severe cortical erosion with extension of uptake into the marrow, suggesting marrow involvement.

COMMENTS

Erdman et al[1] performed ^{99m}Tc WBC SPECT•CT in 77 patients (101 feet) with diabetic foot infection and evaluated the correlation of CSI with outcomes, as well as the impact of duration of antibiotic treatment. Patients with low CSI values (0-2) had a more favorable outcome (treatment failure < 30%), while those with high CSI (7-13) had poor outcomes and prolonged treatment. However, increasing the duration of antibiotic therapy did not achieve better outcomes in patients with CSI more than 7. The only patient group that benefited from increased duration of antibiotic therapy was the group with CSI of 3-6. In this group, the failure rate decreased from 68% to 36% when the duration of antibiotic therapy was increased.
The calculation of CSI thus helps to better define which patients would benefit from prolonged antibiotic therapy and to better predict outcomes. Since defining cortical erosion in the bone and the extent of the infective process is key to proper evaluation of diabetic foot infection, as well as calculation of CSI, this study clearly demonstrates the benefit of the Symbia T2 SPECT•CT with integrated diagnostic CT for such clinical situations. Symbia T2 is able to provide the clarity and sharpness required for the visualization of the smallest diagnostic detail, which enhances visualization of small infective foci.*

EXAMINATION PROTOCOL

Scanner	*Symbia T2*
Dose	***20 mCi autologous ^{99m}Tc WBC***
AC method	***CT-based attenuation correction***
Scan delay	***2 hours post injection delay***
Parameters	***32 frames, 45 sec/frame***
CT	***130 kV, 50 mAs, 1 mm slices***

* Based on competitive informations available at time of publication. Data on file.

4

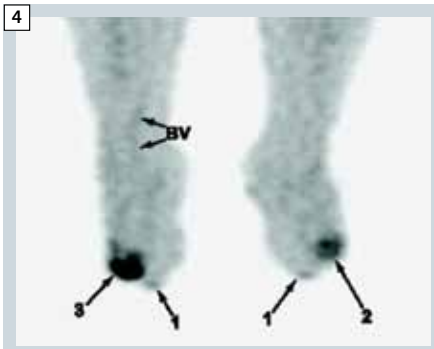

4 A planar image following injection of ^{99m}Tc WBC shows two focal areas of increased uptake in each foot. The focal uptakes with intensity similar to that of the blood vessel (BV) show an intensity score of 1. A lesion on the right foot with intense uptake has an intensity score of 3, while the one in the left foot, which has a slightly lower level of uptake, but is still much higher than that of the blood vessel, has an intensity score of 2.

References:

[1] WILLIAM A. ERDMAN, MD; Diabetes Care. 2012 June 20 Indexing Severity of Diabetic Foot Infection With ^{99m}Tc White Blood Cell Single Photon Emission Computed Tomography/Computed Tomography Hybrid Imaging

5

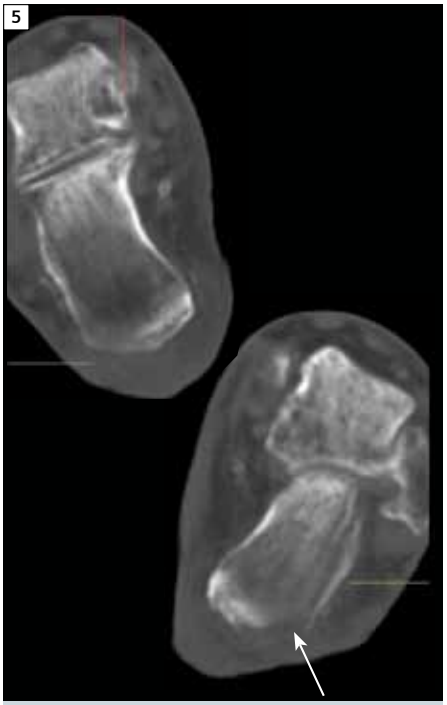

5 CT transverse slice from ^{99m}Tc WBC SPECT•CT in the same patient shows slight erosion of the calcaneus on the left side (white arrow). The calcaneal cortex appears intact on the right side.

6

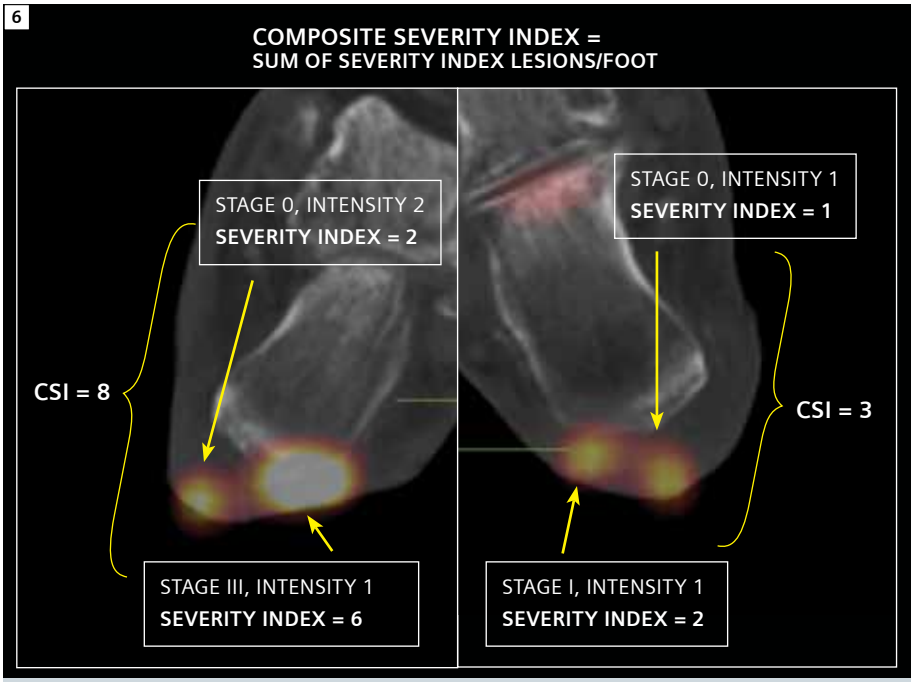

6 Fused SPECT•CT images at the same transverse slice level show two separate infection foci on both feet. Individual stage and intensity scoring and calculation of CSI is demonstrated. The lesion on the left foot with intense uptake and associated cortical erosion with possible extension to marrow has a severity index of 6, while another lesion on the right foot that extends to the calcaneal cortex, but shows no CT change, has a severity index of 2. The summation of the severity index of all lesions in one foot gives the CSI.

Case 3
Primary Carcinoid Tumor in Bronchus Detected by ^{111}In Octreotide SPECT•CT

By Sören Sandström, MD

Case study data provided by Skaraborgs Sjukhus, Skövde, Sweden

HISTORY

A 45-year-old male presented with recurrent cough with occasional hemoptysis. A chest X-ray was negative. Broncoscopy demonstrated a well-delineated tumor mass in the left main bronchus. The thoracic surgeon performing the bronchoscopy suspected a carcinoid based on the appearance of this tumor, which was very prone to bleeding. The patient was referred for Somatostatin receptor scintigraphy with ^{111}In Octreotide SPECT•CT (*Figure 1-2*).

DIAGNOSIS

The patient was referred for surgical removal of the tumor since endoscopic removal of this very vascular lesion was regarded to be too risky. Following surgery, the patient remains symptom-free and all serum parameters, as well as follow-up imaging, has been normal.

1

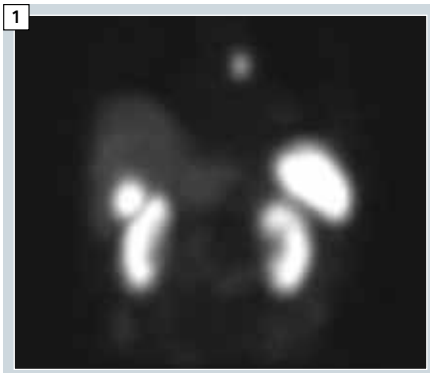

1 A planar image shows focal area of increased uptake in the thorax, which is not possible to localize to the bronchial tumor. Normal tracer accumulation in the liver, gall bladder, spleen and kidneys was visualized.

COMMENTS

Primary bronchial carcinoid tumors are rare and often associated with symptoms of hormone overproduction, especially ectopic ACTH producing tumors causing Cushing's Syndrome.[1] Somatostatin receptor scintigraphy has been widely used[2] for the localization of functioning bronchial carcinoids. One other case report has highlighted the accurate localization of ACTH secreting bronchial carcinoid using ^{111}In Octreotide SPECT•CT, which was not visualized on the planar scan.[3] This case study demonstrates the value of integrated diagnostic CT on the Symbia™ T6 for accurate localization and characterization of the bronchial carcinoid. Advanced reconstruction algorithms on the Symbia T help attain the precise shape of the lesion as delineated in the bronchial lesion. Symbia's fusion with breath-hold thin-slice diagnostic CT was instrumental – not only for proper localization of the endobronchial carcinoid tumor – but also for delineation of tumor extent, lack of infiltration into peribronchial tissue and absence of pneumonitis or lung collapse, which may occasionally complicate such conditions. This also helps manage decision-making and surgical planning.

EXAMINATION PROTOCOL

Scanner	*Symbia T6*
Dose	***6 mCi ^{111}In Octretide***
Scan delay	***24 hours post injection***
Parameters	***60 frames, 30 sec/frame***
CT	***130kV, 30 eff mAs, 3 mm slice***

References:

1 Ectopic ACTH syndrome due to occult bronchial carcinoid. Corsello SM, Fintini D, Lovicu RM, Paragliola RM, Rufini V, Simonetti G, Pontecorvi A. Clin Nucl Med. 2009 Jul;34(7):459-61.

2 Successful application of technetium-99m-labeled octreotide acetate scintigraphy in the detection of ectopic adrenocorticotropin-producing bronchial carcinoid lung tumor: a case report–Esfahani AF, Chavoshi M, Noorani MH, Saghari M, Eftekhari M, Beiki D, Fallahi B, Assadi M. J Med Case Rep. 2010 Oct 18;4:323.

3 Paraneoplastic ACTH secretion: bronchial carcinoid overlooked by planar indium-111 pentetreotide scintigraphy and accurately localized by SPECT/CT acquisition–Aide N, Reznik Y, Icard P, Franson T, Bardet S Clin Nucl Med. 2007 May;32(5):398-400.

2

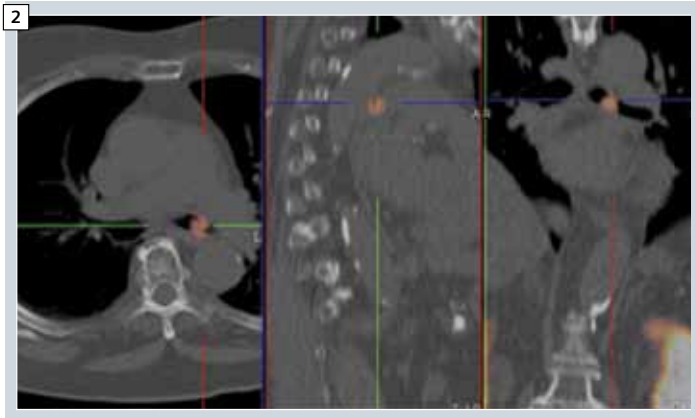

2 SPECT•CT fused images show ^{111}In Octreotide avid tumor in the proximal half of the left bronchus almost blocking the entire bronchial lumen. There was no associated lung collapse or pneumonitis. The tumor does not appear to infiltrate beyond the bronchus.

Case 4
Lymphoscintigraphy SPECT•CT and Sentinel Node Biopsy Using Dual Contrast in a Case of Oral Cancer

By Renato A. Valdés Olmos, MD, PhD

Case study data provided by Netherlands Cancer Institute, Antoni van Leeuwenhoek Hospital, Amsterdam, The Netherlands

INTRODUCTION

Sentinel node detection using lymphoscintigraphy (SNL) followed by biopsy is becoming a standard treatment approach for oral cavity cancer. SNL biopsy is able to select patients with occult metastases so that unnecessary cervical nodal dissection is avoided in a substantial patient population. However, SNL biopsy has a lower sensitivity and negative predictive value for floor of the mouth (FOM) lesions. False negative rates of 25% for FOM tumors have been reported.[1] This may be primarily due to the sentinel nodes being located very close to the primary oral cavity tumors, which can make the detection of sentinel nodes difficult during lymphoscintigraphy due to high tracer level in the primary tumor. Sentinel nodes in close proximity to the primary tumor are also difficult to delineate and separate from the primary tumor during biopsy.

1

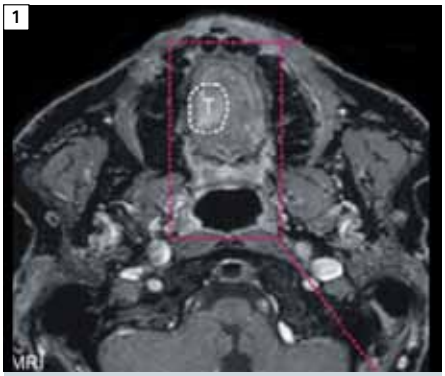

1 MR images delineate the location of the primary tumor, which does not cross the midline.

HISTORY

A 52-year-old female with squamous cell carcinoma in the floor of the mouth was referred for lymphoscintigraphy. SNL biopsy was performed about 6 hours after completion of the SPECT•CT procedure (8 hours following injection of radioactive colloid along with fluorescent Indocyenine Green (ICG)). In the operating room, a pre-incision overview image was acquired using a portable gamma camera. The dissection for sentinel nodes was guided by a handheld gamma probe. Fluorescence imaging was performed during surgery with a handheld fluorescence camera in order to visually detect the SNL containing fluorescent tracer.

DIAGNOSIS

Using gamma probe, three sentinel nodes were identified and excised. All three nodes were also visualized by fluorescence imaging. However, one additional left level 1 sentinel node that was very close to the primary tumor could be identified only by fluorescence imaging, but was impossible to detect separate from the primary tumor by gamma probe.

COMMENTS

This study is a part of a series of 14 patients with oral cavity squamous cell carcinoma evaluated by SPECT•CT lymphoscintigraphy using technetium-99m (^{99m}Tc) Nanocolloid and ICG combination.[2] In all 14 patients, 43 sentinel nodes could be localized intraoperatively by using the combination of a portable gamma camera, a handheld gamma probe and fluorescence imaging. However, in four patients, additional SNL close to the primary tumor were detected only by fluorescence imaging, since localization with handheld gamma devices was not possible for these nodes due to the high radioactive background signal from the primary tumor injection site. Use of such a combined lymphoscintigraphy approach significantly improved the accuracy of surgical excision of SNL by enabling more nodes to be identified intraoperatively and resected.
The Symbia™ SPECT•CT scanner improves sentinel node detection and localization due to the combination of CT morphological information with radiocolloid uptake seen on SPECT. High image resolution related to the Symbia T unique collimator design allows for the highest count rate according to NEMA standards, which helps delineate more sentinel nodes compared to standard lymphoscintigraphy.* Intraoperative localization of SNL is usually guided by handheld gamma ray detection probe. For oral cavity cancers with SNL located close to the primary tumor, localization

of SNL by gamma probe is difficult due to the high radioactive background signal from the injection site in the primary tumor. The near infra-red fluorescent tracer Indocyanine Green (ICG) has been used for intraoperative SNL node localization. ICG is not visible by the naked eye and thus does not interfere with visual identification of tumor boundaries. ICG requires a special fluorescent camera for SNL visualization. However, the drawback of ICG is that it passes through the lymphatic channels quickly, and thereby, has a limited diagnostic window for the detection of SNL.

To compensate for the drawbacks of radioactive colloid (^{99m}Tc Nanocolloid) and fluorescence tracer (ICG), a combination of both tracers for use with lymphoscintigraphy and SPECT•CT with subsequent dual tracer guided SNL biopsy has been demonstrated to be useful as in this case example.

EXAMINATION PROTOCOL

Scanner	*Symbia T6*
Dose	***74 MBq ^{99m}Tc Nanocolloid***
Acquisition	***Dynamic Planar + SPECT•CT***
Scan delay	***2 hours post injection***
Parameters	***64 frames, 20 sec/frame***
CT	***130 kV, 60 mAs, 2mm slices***

2

2 SPECT•CT fused and volume rendered images show a clearly delineated submandibular sentinel node (white arrow) close to the primary tumor injection site. The radioactive node corresponds with a small lymph node in level 1, as seen on CT (white circle).

4

4 Intraoperative fluorescence imaging delineates fluorescent sentinel node. This node was not clearly separable from the radioactive signal from the primary tumor injection site by gamma probe. Fluorescence imaging ensured accurate intraoperative SNL localization and resection. All the excised sentinel nodes were demonstrated to be free of micrometastases by histopathology. In view of the node negative status, the patient was advised resection of primary tumor, but without extended neck node dissection.

3

3 An intraoperative planar scintigraphic image obtained by portable gamma camera prior to excision shows very high uptake in the primary tumor injection site without proper visualization of radioactive sentinel nodes due to excessive radioactivity in the primary injection site. Following the masking of the primary tumor injection site, radioactive sentinel nodes are visualized (white arrows). Following the excision of the sentinel nodes, another intraoperative planar scintigraphic image with the primary tumor masked shows an absence of tracer in the sentinel node sites, which suggests that the nodes have been excised.

* Based on competitive information available at time of publication. Data on file.

References:

[1] Civantos et al J Clinic Oncol 2012; 28(8):1395-400

[2] Nynke S van den Berg et al EJNM 2012; 39:1128-1136

Case 5

SPECT•CT-based Delineation of Metastatic Node Not Visualized on Planar Lymphoscintigraphy in a Case of Melanoma

By Dr. Michael Hofman, MBBS, FRACP

Case study data provided by Peter MacCallum Cancer Centre, Melbourne, Australia

HISTORY

An elderly patient presented with melanoma in the scalp without clinically palpable neck node metastases. SPECT•CT lymphoscintigraphy was performed on Symbia™ T6 (*Figures 1-3*).

In order to better understand the nature of the enlarged node, the patient also underwent Fludeoxyglucose F 18* (^{18}F FDG) PET•CT (*Figure 4*).

1

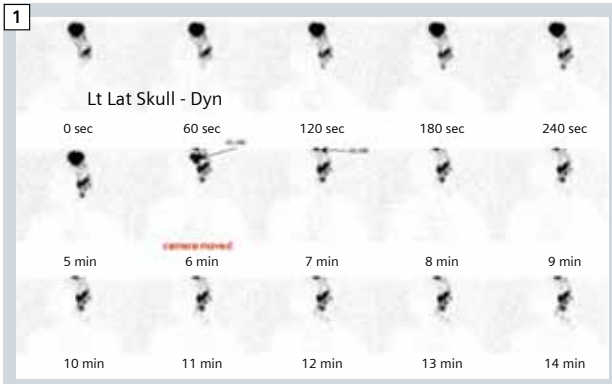

1 Planar dynamic images following peritumoral injection demonstrate radiolabeled nanocolloid retention in the sentinel lymph nodes in the neck.

2

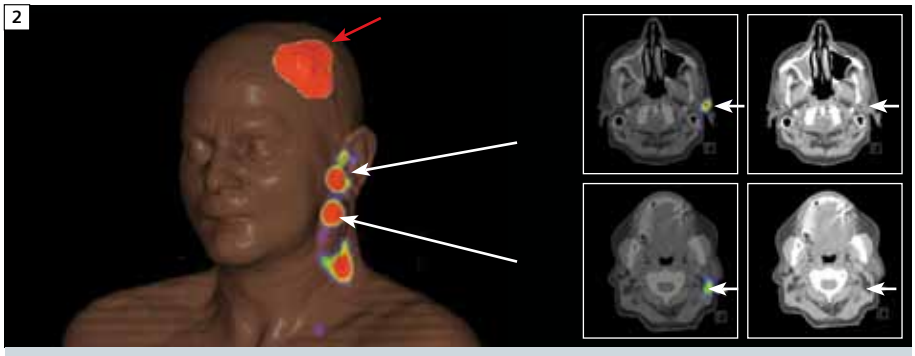

2 Surface volume rendering of the fused SPECT•CT data shows tracer uptake in the scalp melanoma related to peritumoral injection of radiolabeled colloid (red arrow). Ipsilateral sentinel nodes in the upper, mid and lower cervical nodal groups show focal tracer uptake. A comparison of SPECT•CT fused images and corresponding CT images helps delineate small preauricular sentinel node and level II (jugulodigastric) secondary tier nodes (white arrows).

DIAGNOSIS

SPECT•CT Lymphoscintigraphy and PET•CT of neck confirmed presence of metastatic node in the cervical lymph nodal chain, which suggests more advanced disease stage.

COMMENTS

The findings from the Symbia T SPECT•CT study changed case management significantly. Without it, the sentinel pre-auricular node would be targeted for excision without knowledge of the macroscopic malignant node situated further inferiorly. The presence of macroscopic node replacement also represents stage III disease, which confers an adverse prognosis and may guide adjuvant therapy. Delineation of enlarged cervical lymph node in absence of radioactive colloid uptake was made possible by the integrated CT performed as a part of the SPECT•CT lymphoscintigraphy. Impact of CT in SPECT•CT lymphoscintigraphy is thus not only for localization of tracer avid sentinel nodes, but also for proper characterization of nodes, and other soft tissue lesions including enlarged non tracer avid nodes, which may harbour metastases as this case amply demonstrates. Symbia T advanced reconstruction and highest NEMA sensitivity** allows for small lesions to be reconstructed with more counts in the correct volume, which increases contrast for improved delineation of small nodes.

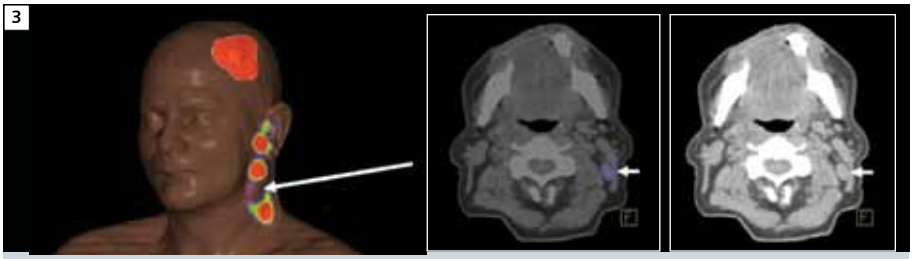

3 An enlarged cervical lymph node visualized on CT, but without significant uptake of ^{99m}Tc Nanocolloid (white arrow), suggests the possibility of an enlarged node with malignant cells but without radiocolloid uptake. This may be related to malignant infiltration of the node, so that it is no longer functioning as normal lymphatic tissue and is, therefore, accumulating very little nanocolloid.

The reliability of sentinel node biopsy is dependent on the accurate visualization and identification of the sentinel node during lymphoscintigraphy. Extensive metastatic involvement of a sentinel node can lead to blocked inflow and rerouting of lymphatic drainage to a different adjacent sentinel node that may not contain tumor cells. This may lead to a false negative sentinel node biopsy. Identification of enlarged nodes in the sentinel nodal pathway using Symbia T with integrated CT may help define such sentinel nodes with extensive malignant infiltration. Similar findings have been shown in SPECT•CT lymphoscintigraphy in other tumor sites. Leitje[1] performed SPECT•CT lymphoscintigraphy in 17 patients with penile cancer with palpable inguinal lymph nodes which were biopsy proven as metastases. Thirteen out of 17 palpable inguinal nodes did not show uptake of radioactive colloid. In 10 of these nodes, rerouting of lymphatic drainage to a neo-sentinel node was demonstrated. In one case, rerouting of lymphatics was to the contralateral inguinal region. In all cases, the enlarged nodes were delineated on integrated CT, which suggests its value in delineating such nonvisualized metastatic nodes during lymphoscintigraphy and may guide appropriate nodal sampling and reduce false negatives.

Nonvisualization of sentinel nodes may be related to poor technique and patient related factors like obesity, etc. However, presence of metastatic nodes leading to blockage of lymphatic flow is sometimes linked with sentinel node nonvisualization during lymphoscintigraphy. Brenot-Rossi[2] found nonvisualized axillary sentinel nodes in 30 out of 332 patients with breast cancer. A total of 63.3% of patients with nonvisualized axillary sentinel nodes (blocked axillary lymphatic drainage) were positive for axillary nodal metastases. This was far higher than that for patients with well visualized axillary SNL (28.5%). Such findings further suggest the value of integrated CT in lymphoscintigraphy in patients with nonvisualization of sentinel nodes.

EXAMINATION PROTOCOL

Scanner	*Symbia T6*
Dose	***74 MBq ^{99m}Tc Nanocolloid***
Acquisition	***Dynamic Planar + SPECT•CT***
Scan delay	***1 hour post injection***
Parameters	***64 frames, 20 sec/frame***
CT	***130 kV, 60 mAs, 2mm slices***

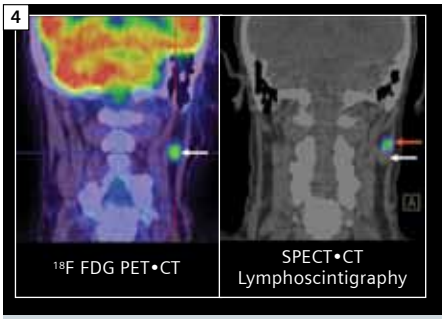

4 ^{18}F FDG shows increased glycolytic activity in the enlarged cervical lymph node, which does not show uptake of radioactive nanocolloid in the SPECT•CT lymphoscintigraphy image (white arrows). Note the uptake of nanocolloid in the sentinel node (red arrow) just above the enlarged FDG avid cervical node. This confirms that the enlarged lymph node is metastatic and completely infiltrated with malignant cells without significant normal lymphoid tissue, which explains the absence of nanocollid uptake. Ultrasound-guided fine needle aspiration (FNA) of the node also confirmed malignant melanoma.

Indications

Fludeoxyglucose F 18 Injection is indicated for positron emission tomography (PET) imaging in the following settings:

- **Oncology:** For assessment of abnormal glucose metabolism to assist in the evaluation of malignancy in patients with known or suspected abnormalities found by other testing modalities, or in patients with an existing diagnosis of cancer.
- **Cardiology:** For the identification of left ventricular myocardium with residual glucose metabolism and reversible loss of systolic function in patients with coronary artery disease and left ventricular dysfunction, when used together with myocardial perfusion imaging.
- **Neurology:** For the identification of regions of abnormal glucose metabolism associated with foci of epileptic seizures.

Important Safety Information

- **Radiation Risks:** Radiation-emitting products, including Fludeoxyglucose F 18 Injection, may increase the risk for cancer, especially in pediatric patients. Use the smallest dose necessary for imaging and ensure safe handling to protect the patient and health care worker.
- **Blood Glucose Abnormalities:** In the oncology and neurology setting, suboptimal imaging may occur in patients with inadequately regulated blood glucose levels. In these patients, consider medical therapy and laboratory testing to assure at least two days of normoglycemia prior to Fludeoxyglucose F 18 Injection administration.
- **Adverse Reactions:** Hypersensitivity reactions with pruritus, edema and rash have been reported; have emergency resuscitation equipment and personnel immediately available.

* The full prescribing information for fludeoxyglucose F 18 injection can be found on pages 43-45.

** Based on competitive informations available at time of publication. Data on file.

References:
[1] J Nucl Med 2009; 50:364–367
[2] J Nucl Med. 2003 Aug; 44(8): 1232-7

Case 6
Subperiosteal Hematoma Characterized by SPECT•CT

By William Pavlosky, MD and Jozef Nycz, CNMT

Case study data provided by Timmins and District Hospital, Ontario, Canada

HISTORY

A 78-year-old female presented with pain in the left thigh, with a duration of a few weeks. The patient did not recall any specific incidence of trauma. Initial X-ray images were normal. Patient was referred for a technetium-99m methylenediphosphonate (^{99m}Tc MDP) bone SPECT•CT study.

DIAGNOSIS

The dystrophic calcification was suggestive of trauma or soft tissue infective process. To clarify the etiology, an MRI was performed (*Figures 3-4*).
The patient was treated conservatively with clinical and MRI-based follow-up.

COMMENTS

SPECT•CT with integrated diagnostic CT performed on the Symbia™ T16 was instrumental in the diagnosis of subperiosteal hematoma. SPECT•CT indicated that the focal area of increased skeletal metabolism was confined to the periosteum of the femoral shaft with slight extension into adjacent soft tissue, which corresponded to the focal hyperintensity within the vastus muscle demonstrated on integrated thin-slice diagnostic CT. Absolute precision of fusion is essential for the determination of the origin of uptake in such situations, as demonstrated by the precise fusion of SPECT and CT by Symbia T16. MRI and ultrasound were confirmatory, but not essential for the diagnosis, for which SPECT•CT was adequate. The high-resolution, thin-slice diagnostic CT component of Symbia T16, however, was critical for diagnosis because it demostrated the fine detail in the periosteal region and adjacent muscle, which clearly defined the fine linear hyperintensity that coregistered exactly to the focal uptake of ^{99m}Tc MDP.

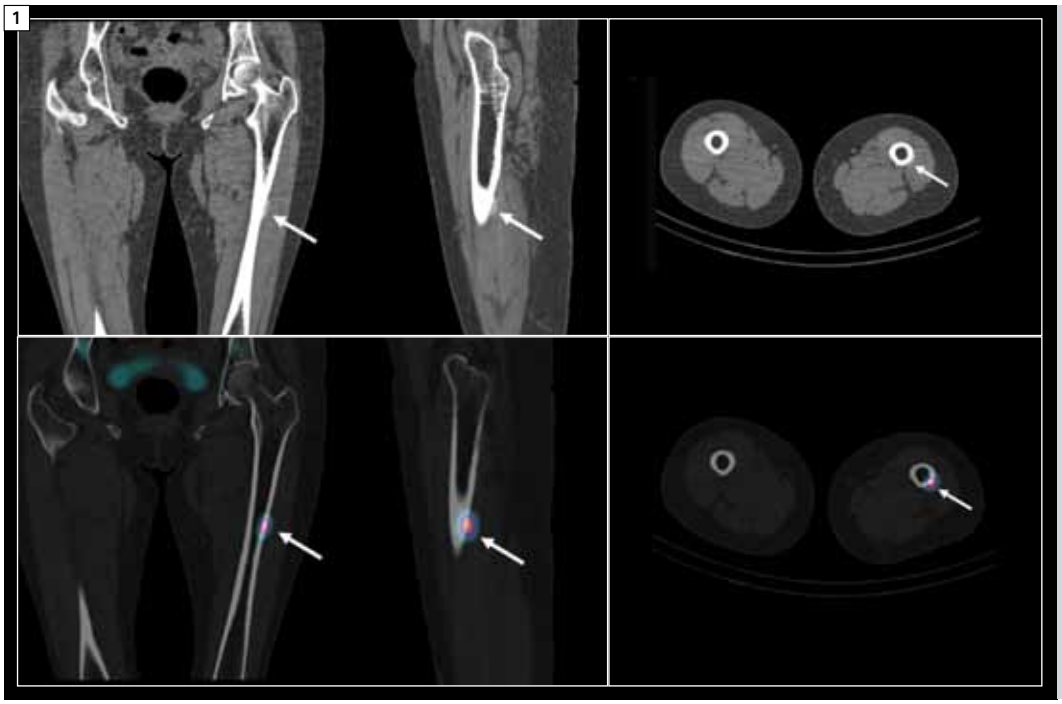

1 The SPECT•CT study shows focal uptake of tracer in the posterolateral aspect of the middle of shaft of the left femur, localized to the cortex, but extending to the adjacent soft tissue. Integrated thin-slice diagnostic CT demonstrated focal hyperdensity in the vastus muscle adjacent to the periosteum of the femoral shaft, which corresponded exactly to the focal uptake of ^{99m}Tc MDP seen on SPECT. Uptake of tracer within the CT hyperintensity is suggestive of dystrophic calcification within the muscle adjacent to the periosteum.

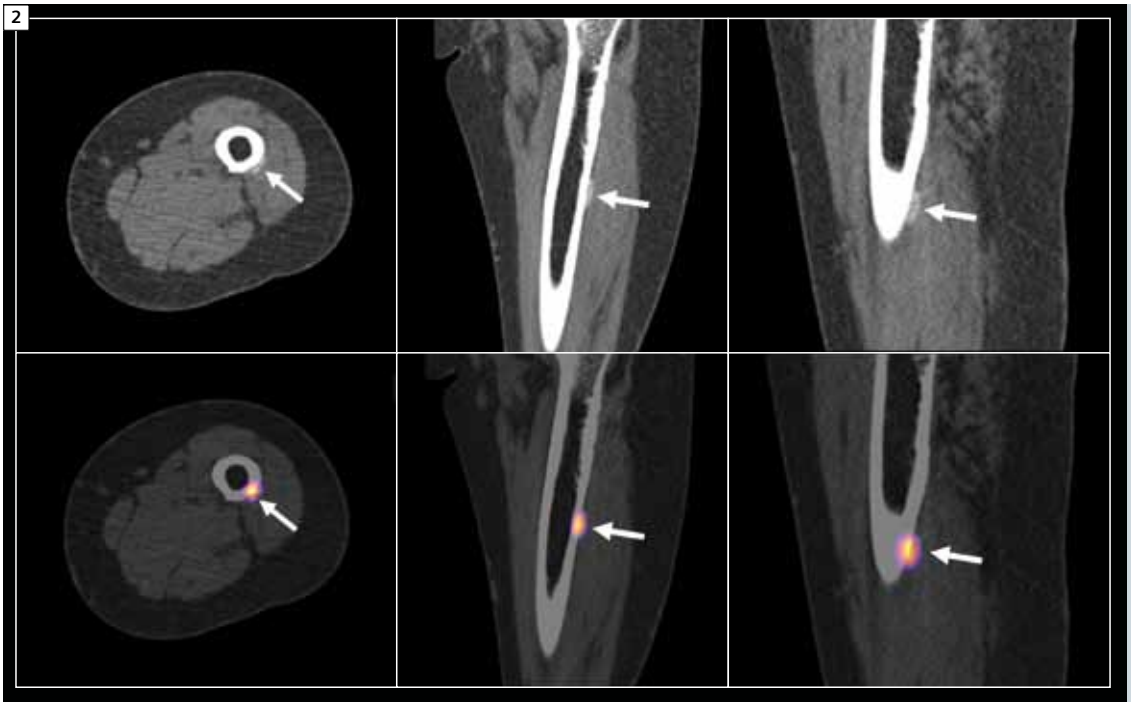

2 A zoomed view of the femoral shaft and adjacent musculature demonstrates the dystrophic calcification in the muscle adjacent to the periosteum of the femoral shaft, with uptake of tracer exactly corresponding to the calcification and the adjacent cortex of the femur. No other region of abnormal uptake is visualized. The femoral cortex and marrow cavity appear normal on CT.

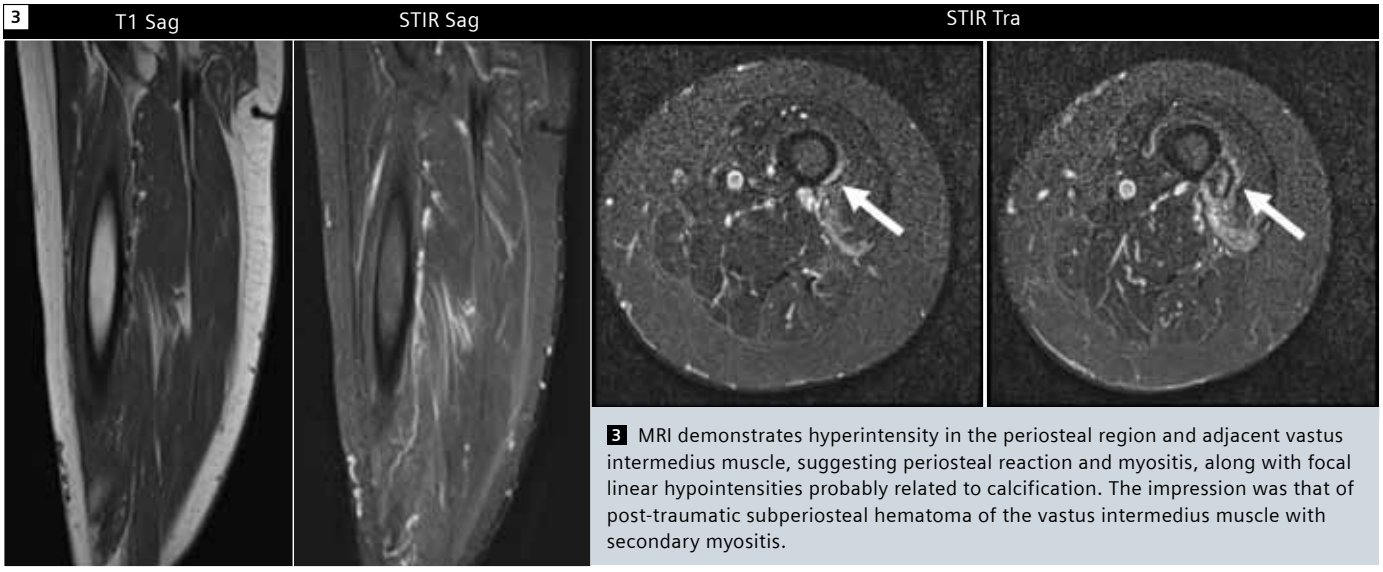

3 MRI demonstrates hyperintensity in the periosteal region and adjacent vastus intermedius muscle, suggesting periosteal reaction and myositis, along with focal linear hypointensities probably related to calcification. The impression was that of post-traumatic subperiosteal hematoma of the vastus intermedius muscle with secondary myositis.

EXAMINATION PROTOCOL

Scanner	*Symbia T16*
Dose	***20 mCi ^{99m}Tc MDP***
Scan delay	***3 hours post injection***
Parameters	***64 frames, 20 sec/frame***
CT	***130 kV, 30 eff mAs, 3 mm slices***

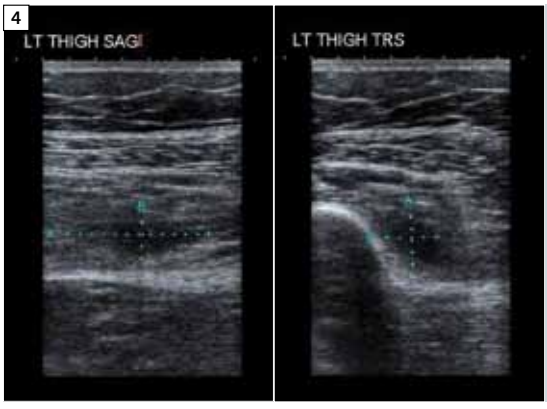

4 The patient also had an ultrasound of the thigh that confirmed the presence of subperiosteal hematoma, as demonstrated by the hypoechoic zone in the muscle plane.

Case 7
SPECT•CT Characterization of Giant Cell Tumor in the Femoral Condyle

By Ashley Hamilton

Case study data provided by Dr. Everett Chalmers Regional Hospital, Fredericton, NB, Canada

HISTORY

A 43-year-old man presented with left knee pain following a soccer injury. X-ray showed a cystic lesion in the left medial femoral condyle. The patient was referred for a technetium-99m methylenediphosphonate (^{99m}Tc MDP) bone SPECT•CT study.

DIAGNOSIS

Scans from the Symbia™ T6 show increased skeletal metabolism within the cystic lesion in the anterior half of the medial condyle of the left femur in the lower and anterior aspect (*Figure 1*). The cystic lesion measures 4 cm x 2.5 cm x 3 cm on CT.
The high-resolution CT obtained from Symbia T16 shows a well-defined border of the cystic lesion with a thin rim of sclerosis. The lesion involves both the distal femoral metaphysis and the epiphysis with extension into the subchondral region.

COMMENTS

The appearance of the cyst, the irregular internal margin, thin rim and ground glass appearance within the cyst seen on CT suggest the diagnosis of a giant cell tumor. Aneurysmal bone cyst or eosinophilic granuloma are also possibilities. The trauma-related pathological fracture in the cyst margin involving part of the patello-femoral surface with increased skeletal metabolism clearly delineated the site and cause of the left knee pain. The cyst would probably have gone undetected without the trauma-related pathological fracture and related pain.

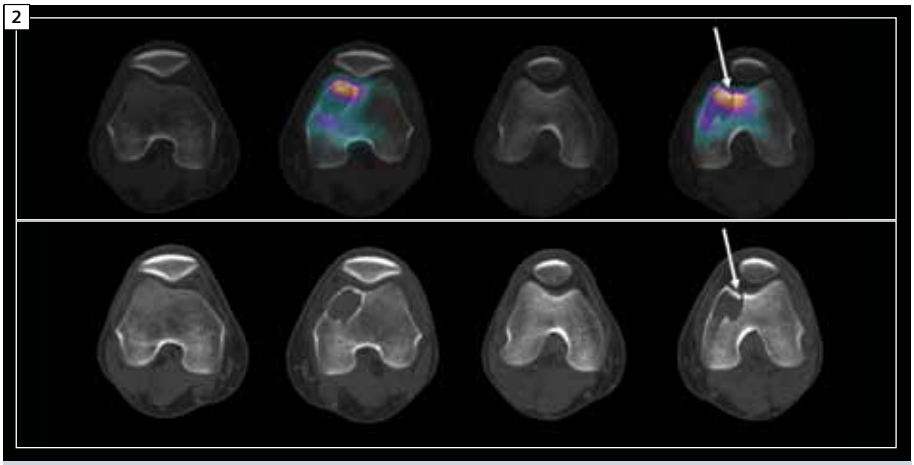

2 Transverse CT and fused SPECT•CT images show a cystic lesion in the anterior part of the right medial femoral condyle with associated fracture in the anterior margin of the cyst (white arrow), which also corresponds to the area of maximum uptake of ^{99m}Tc MDP related to increased skeletal metabolism secondary to the traumatic fracture of the cyst margin. The fracture fragment was displaced inward by 4 mm as delineated on CT. The fracture fragment involves a part of the patello-femoral articular surface (white arrow). The cyst shows a ground glass appearance on CT. High resolution of the Flash SPECT reconstruction, as well as thin- slice, high-quality CT, enhances the visualization of the fractured cyst margin.

EXAMINATION PROTOCOL

Scanner	*Symbia T16*
Dose	***20 mCi ^{99m}TC MDP***
Parameters	***64 frames, 20 sec/frame***
CT	***130 kV, 60mAs, 3 mm slice***

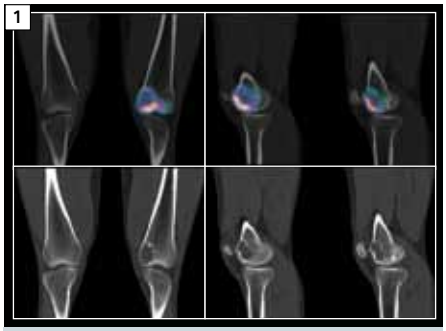

1 SPECT•CT shows uptake within a portion of femoral cystic lesion.

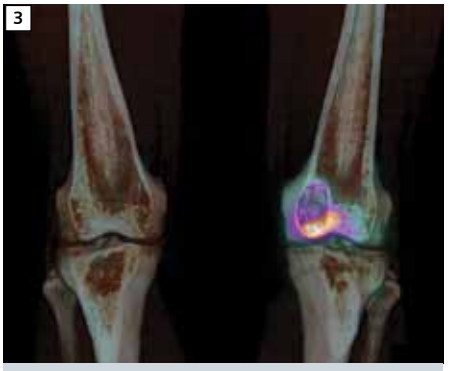

3 A volume-rendered fused SPECT•CT image shows the relationship of the cyst and the fracture site to the articular surface. Despite the benign nature of the giant cell tumor, the presence of a fracture fragment involving the patello-femoral joint surface may complicate recovery and restoration of complete knee joint motion.

Case 8
Characterization of Pelvic Uptake of ^{131}I in a Patient with Thyroid Carcinoma

By Carlos Anselmi, MD, Daniela Fernandez, MD and Osvaldo Estrela Anselmi, MD

Case study data provided by Santa Casa Hospital, Porto Alegre, Brazil

HISTORY

A 66-year-old woman with a history of papillary carcinoma of the thyroid underwent near total thyroidectomy and was further treated with radioiodine ablation therapy with 100 mCi ^{131}I. An ^{131}I whole-body scan was performed 18 days after the administration of ^{131}I. A SPECT•CT study of the pelvis with integrated diagnostic CT for lesion localization and attenuation correction was performed on a Symbia™ T2 system.

DIAGNOSIS

The focal uptake within the bowel lumen was deemed to be related to activity inside a colonic diverticulum. The patient was reassured about the benign nature of the pelvic focal uptakes and put on clinical follow-up.

COMMENTS

Focal uptake of ^{131}I in the uterus is commonly related to iodine retention in the menstruating uterine wall,[1] although one case report has demonstrated ^{131}I uptake in a uterine leiomyoma.[2] Similarly, radioiodine uptake has been reported in intestinal and esophageal diverticula[3] that may mimic metastatic disease. Improved localization and associated anatomical information obtained from the Symbia T2 with integrated diagnostic CT helps with the accurate characterization of such abnormal focal uptake of ^{131}I not related to metastases, as demonstrated in this case within the uterus, and colonic diverticulum further illustrate the value of Symbia T with integrated CT for ^{131}I scintigraphy in thyroid carcinoma.

EXAMINATION PROTOCOL

Scanner	*Symbia T2*
Dose	***100 mCi ^{131}I therapy dose***
Acquisition	***Whole body Planar + SPECT•CT***
Scan delay	***18 days post administration***
Parameters	***64 frames, 30 sec/frame***
CT	***130 kV, 40 eff mAs, 5 mm slices***

References:

1 Rachinsky et al Iodine-^{131} uptake in a menstruating uterus: value of SPECT/CT in distinguishing benign and metastatic iodine-positive lesions. Thyroid. 2007 Sep;17(9):901-2

2 Hirata et al Radioiodine therapy for thyroid cancer depicted uterine leiomyoma. Clin Nucl Med. 2009 Mar;34(3):180-1

3 Nguyen et al Epiphrenic diverticulum: potential pitfall in thyroid cancer iodine-^{131} scintigraphy Clin Nucl Med. 2005 Sep;30(9): 631-2

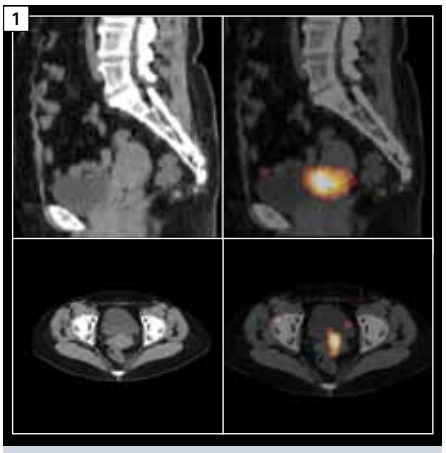

1 Focal uptake of ^{131}I in the pelvis localized to the uterus with integrated diagnostic CT. Uptake in the uterus was deemed to be related to uterine mucosal uptake during menstruation.

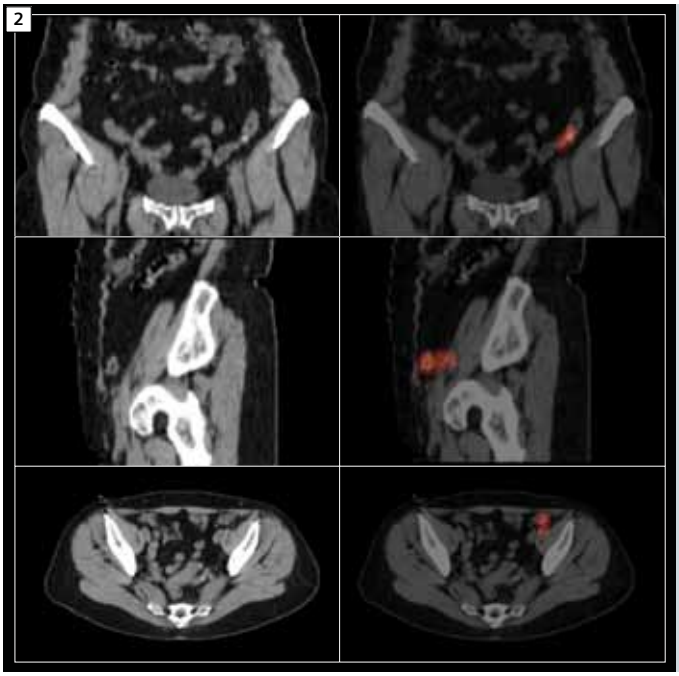

2 Another focal pelvic uptake of ^{131}I was localized to a bowel loop due to integrated diagnostic CT. Diagnostic CT with subsecond rotation delivered motion free images of bowel loops, which could clearly localize the abnormal uptake to be within a bowel loop (probably sigmoid loop). This was deemed to be related to activity inside a colonic diverticulum. The patient was reassured about the benign nature of the pelvic focal uptakes and put on clinical follow-up.

Case 9
SPECT•CT Delineation of Infection in Bone Graft Site

By William Pavlosky, MD and Jozef Nycz, CNMT

Case study data provided by Timmins and District Hospital, Ontario, Canada

HISTORY

A 35-year-old male presented with slowly progressing pain in the right hip. Initial X-ray and bone scan (*Figure 1*) performed in 2004 demonstrated a sclerotic lesion in right femoral neck, which indicated focal skeletal hypermetabolism. The femoral lesion was deemed a benign osteoma. Patient underwent surgery in May 2008 for a bone graft implantation and fixation with nail, plate and compression screws (*Figure 2*). The nail and screws were subsequently removed.
The patient complained of persistent pain in the hip and underwent a bone scan in September 2010.
The planar bone scan (*Figure 3*) showed a mild increase in skeletal metabolism in the right lesser trochanter and neck. Although the uptake pattern was nonspecific, based on the previous history of surgery and bone graft implantation, the possibility of low grade infection at the site of screw removal was considered.

1 Bone scan, 2004 X-ray, 2004

2 X-ray and CT images show nail and plate.

DIAGNOSIS

The bone SPECT•CT (*Figure 4*) showed a mild increase in uptake of technetium-99m (^{99m}Tc) MDP in the neck, lesser trochanter and upper part of shaft of the right femur, corresponding to hyperintense areas of bone graft placement and sclerosis as seen on integrated thin-slice diagnostic CT. Gallium-67 (^{67}Ga) SPECT (*Figure 5*) shows increased uptake in the neck and upper part of shaft of the right femur corresponding to the site of nail insertion.
SPECT•CT (*Figure 6*) localizes increased ^{67}Ga uptake to the region of hyperintensity related to bone graft material in the femoral trochanter as well as in the site of compression screw removal. Gallium uptake corresponds to the region of mild ^{99m}Tc MDP uptake, although the gallium uptake is more intense, suggesting infection in the site of nail and screw removal.
The patient was treated conservatively with aggressive antibiotics, and a follow-up CT was performed in January 2011. CT (*Figure 7*) showed hyperintensity related to the bone graft material and minor sclerosis in the margins of the tunnel created following removal of the nail and screws. No pathological fractures or exaggerated osteolysis was visualized.
The patient further underwent an MRI in July 2011 (*Figure 8*), which demonstrated contrast enhancement in the region of the bone graft material, surgical tunnel, side plate and screw sites. The enhancement pattern was nonspecific and a follow-up bone and Gallium scan was recommended to evaluate for the presence or progress of infection.
With the highest NEMA sensitivity rate,* the Symbia T delivers high SPECT•CT image quality, which was instrumental in appropriate comparison of bone and gallium SPECT•CT images.

3 Planar bone scan, Sept. 2010

4 ^{99m}Tc MDP Bone SPECT•CT, Dec. 2010

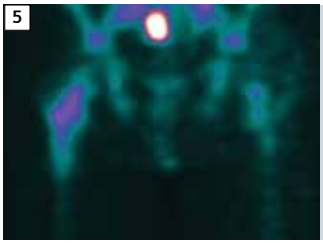

5 ^{67}Ga SPECT•CT, Dec. 2010

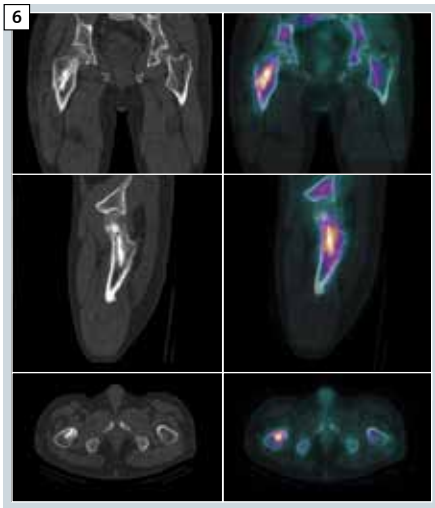

6 ^{67}Ga SPECT•CT, Dec. 2010

COMMENTS

This study clearly demonstrates the comprehensive nature of evaluation using Symbia™ T SPECT•CT for such complicated postoperative situations where the presence of infection can only be evaluated by metabolic imaging. Although the degree of skeletal hypermetabolism was low, the presence of low grade infection at the site of the nail and screw removal in the femoral neck, trochanter and shaft was clear from the gallium scan. However, the integrated diagnostic CT component of the Symbia T clearly localized the infection to the site of bone graft material and the margins of the bony tunnel created following the nail and screw removal. Thin-slice CT obtained from the Symbia T also clarified the absence of pathological fracture and associated bony pathology. Subsequent CT and MRI were nonspecific regarding the presence of infection and only bone and gallium scan-based follow-up was of any clinical value.

EXAMINATION PROTOCOL

Scanner	*Symbia T*
Dose	***20 mCi ^{99m}Tc MDP***
Parameters	***64 frames, 15 sec/frame***
Recon	***Flash***
CT	***130 kV, 50 eff mAs, 3 mm slice***

7 CT shows sclerosis in tunnel margin.

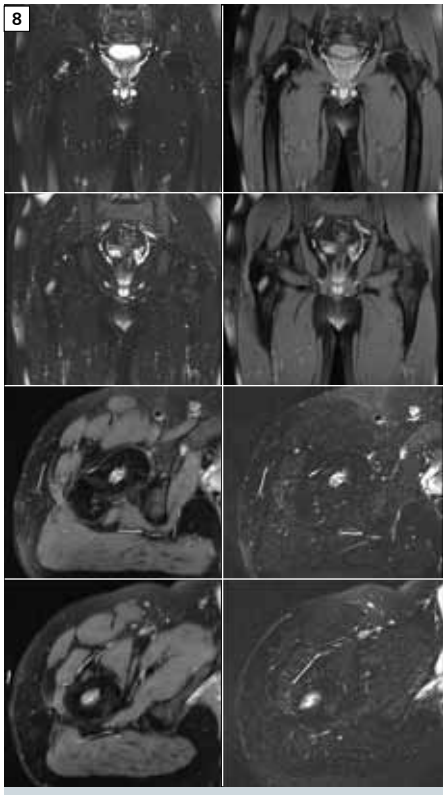

8 MRI Post Contrast, July 2011

* Based on competitive informations available at time of publication. Data on file.

Case 10

Precise Localization of a ‘Hot Screw’ After Total Knee Replacement Demonstrated by SPECT•CT

By Robert Cooper, MD, Stephen Allwright, MD and Dale L. Bailey, PhD

Case study data provided by The Mater Hospital, Royal North Shore Hospital and the University of Sydney, Sydney, Australia

INTRODUCTION

SPECT•CT has proven to be useful in helping physicians enhance diagnostic accuracy when compared with conventional SPECT, particularly in bone scanning (*Figures 1-2*). This case demonstrates the improved accuracy of localization of the exact cause of the patient’s symptoms using integrated diagnostic CT combined with SPECT.

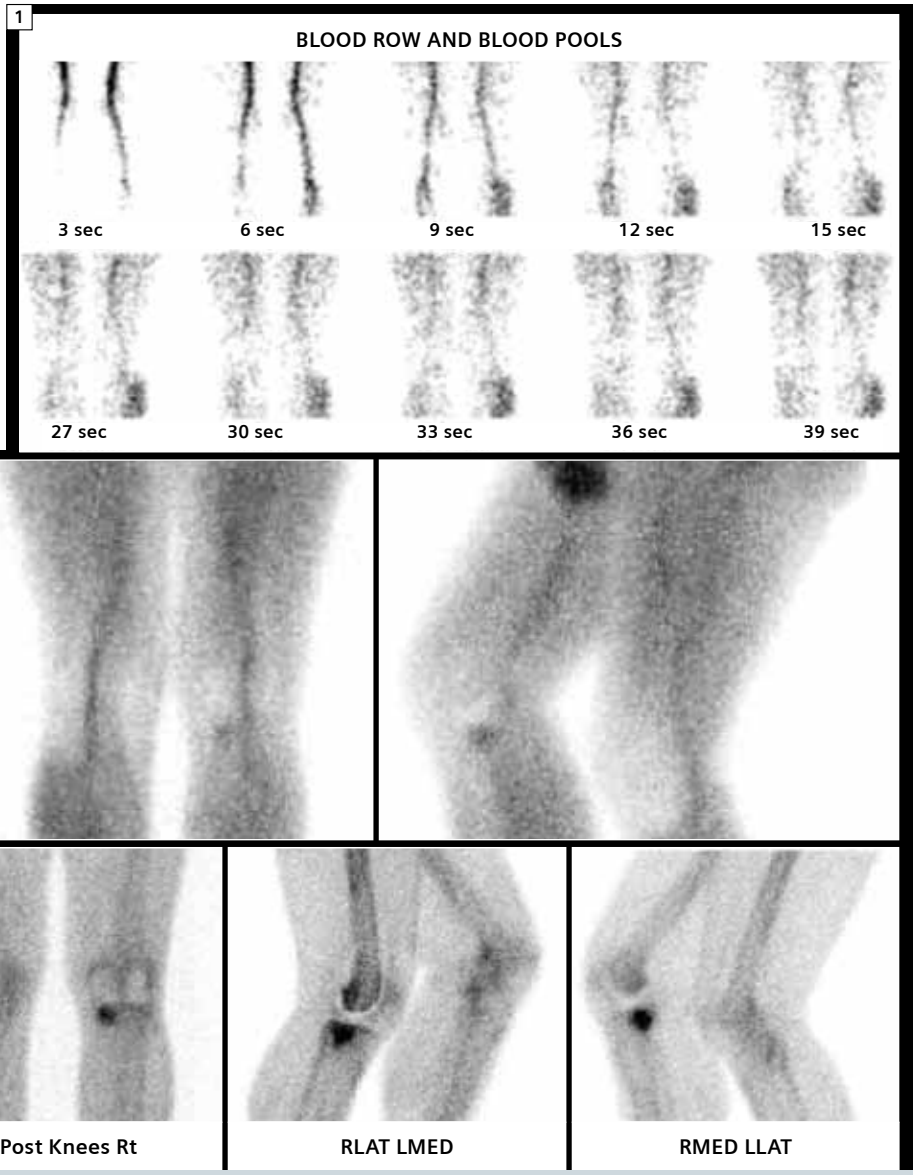

1 Dynamic blood flow, blood pool and planar spot views of knee joints.

2

2 SPECT•CT study shows focal uptake in single prosthetic screw.

HISTORY

A 65-year-old male received a total knee replacement in 2005. Although he initially had good results, the knee became progressively painful over a few years. Various imaging scans did not indicate the cause of the pain. A three-phase limited bone scan was performed in March 2010. Imaging was commenced immediately after the injection of ~800 MBq of technetium-99m methylenediphosphonate (^{99m}Tc MDP). A dynamic acquisition over the lower femurs and knees was acquired followed by multiple static blood pool planar images and 3-hour delayed views. This was followed by a SPECT•CT scan performed on a Symbia™ T.

DIAGNOSIS

The initial dynamic scan (*Figure 1*) showed increased soft tissue perfusion to the lower contralateral limb, presumably due to altered weight bearing. The blood pool images that followed immediately demonstrated a small focus of increased vascularity on the medial side of the right knee. The planar delayed views 3 hours later showed intense uptake on the medial side of the right tibia related to the right knee prosthesis. The SPECT•CT scan (*Figure 2*) showed increased uptake localized to the postero-medial tibial screw with no abnormal uptake elsewhere around the prosthesis. The possible causes for this include an infected screw, screw loosening or screw osteolysis. High SPECT resolution achieved by Symbia T with Flash enhances delineation of small foci of screw loosening.

In May 2010, a revision of the knee replacement was performed with the tibial plate, and the postero-medial screw was replaced. Postoperatively, the patient had markedly reduced pain postero-medially in the knee.

COMMENTS

This case demonstrates the exquisite localization capabilities of the Symbia T with integrated diagnostic CT in spite of the limited spatial resolution of the SPECT study. Without the integrated diagnostic CT, the focus of uptake in the right knee would have been equally visible, but the ability to localize it to a single screw would not have been as certain. Fusion images defining the exact lesion location significantly helped manage decision-making and surgical planning. In view of the limited nature of the uptake confined to a single screw within the prosthesis, a loosening of the screw was regarded as the most plausible explanation of the patient's progressive pain.

EXAMINATION PROTOCOL

Scanner	*Symbia T*
Dose	***20 mCi ^{99m}Tc MDP***
Parameters	***64 frames, 15 sec/frame***
Recon	***Flash***
CT	***130 kV, 30 eff mAs, 3 mm slice***

References:

1 Roach PJ, Schembri GP, Ho Shon IA, Bailey EA, Bailey DL. SPECT/CT imaging using a spiral CT scanner for anatomical localization: Impact on diagnostic accuracy and reporter confidence in clinical practice. Nucl Med Commun. 2006 Dec;27(12):977-987

2 Schillaci O. Hybrid SPECT/CT: a new era for SPECT imaging? Eur J Nucl Med Mol Imaging. 2005 May;32(5):521-524

Case 11
Peroneal Compartment Syndrome Characterized by ^{99m}Tc MDP Bone SPECT•CT

By Ashley Hamilton

Case study data provided by Dr. Everett Chalmers Regional Hospital, Fredericton, NB, Canada

HISTORY

A 29-year-old male presented in the emergency room with severe right lower leg pain with extreme tenderness in the fibular region. He was serving in the military and was running 10 km every day as part of training. The pain started 2 days prior to the ER visit and was increasing progressively. Clinical examination showed no swelling or redness in the affected limb. No apparent fracture was seen on X-ray.

1

1 Planar bone image.

2

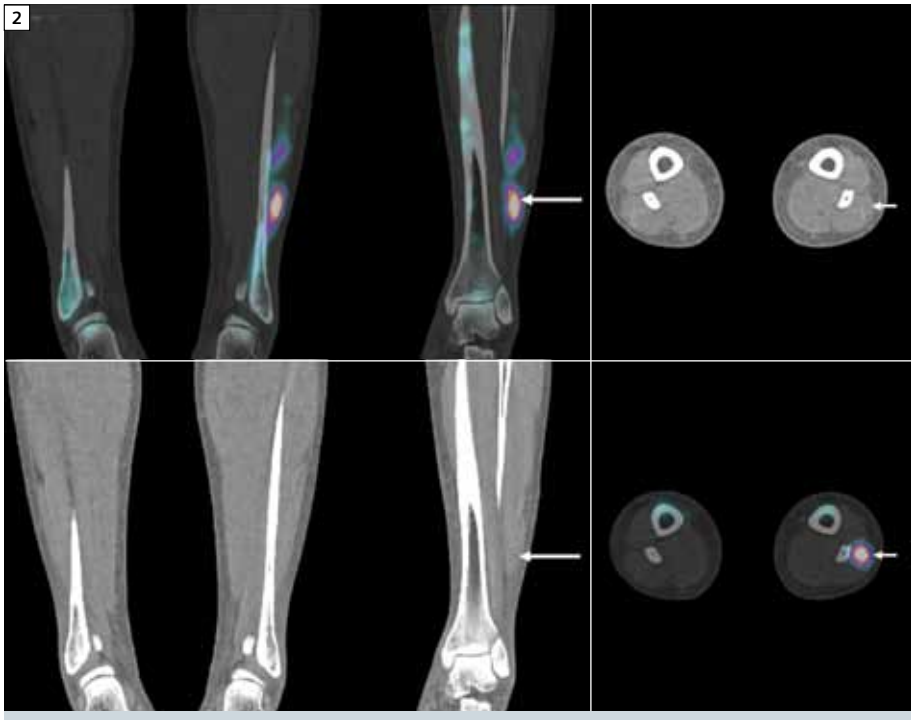

2 SPECT•CT images show increased uptake in left peroneal muscles.

DIAGNOSIS

Planar bone scan images show asymmetric increase in technetium-99m methylenediphosphonate (^{99m}Tc MDP) uptake in the posterolateral aspect of the left leg from the midpoint to just distal of the ankle (*Figure 1*). The activity is linear and slightly irregular, located in the vicinity of the fibula with an atypical appearance not directly correlating with a fibular uptake. The right leg (site of symptoms) does not show any abnormal uptake except a mild increase in tibial cortical uptake.

Scans taken on a Symbia™ T16 SPECT•CT scanner with integrated diagnostic CT demostrate that the abnormal accumulation of tracer, in fact, does not correspond to the left fibula, but is located within the soft tissue of the lateral compartment in the vicinity of the peroneus brevis and peroneus longus muscles (*Figure 2*). The uptake extends lateral and inferior to the fibula and, at the inferior level, the uptake is posterior to the fibula, following the path of the peroneal compartment. The SPECT•CT appearance was suggestive of a myositis or compartment syndrome secondary to trauma. The right lower leg does not show any abnormal tracer uptake, although CT shows small streaks of slightly increased intensity in the right peroneal muscles.

In view of the confusing discrepancy between clinical symptoms (right leg pain) and the SPECT•CT findings (left peroneal compartment soft tissue

uptake), the patient underwent MRI of the lower limbs, and MRI images were fused with the SPECT images for optimum evaluation.
MRI images (*Figure 3*) show mild edema in the left peroneus muscles lateral to left fibula corresponding to the region of increased tracer uptake in the SPECT images (white arrows). T2 and STIR images show slight hyperintensity reflecting muscle edema, mild swelling and myositis within the peroneal muscles. There is no uptake of Gd contrast within the lesion. In the peroneal longus on the right leg, there is a prominent localized increase in signal, particularly demonstrated in axial T1 Fat Sat sequences, within a lengthy segment of the muscle, which was felt to be most likely due to hemorrhage. Post-contrast sequences did not show much hypervascularity or retention of Gd within the right peroneus musculature. T2 sequences also demonstrated hyperintensity in the peroneus muscles, as well as the adjacent soleus muscle, with slight fluid tracking along fascial planes.

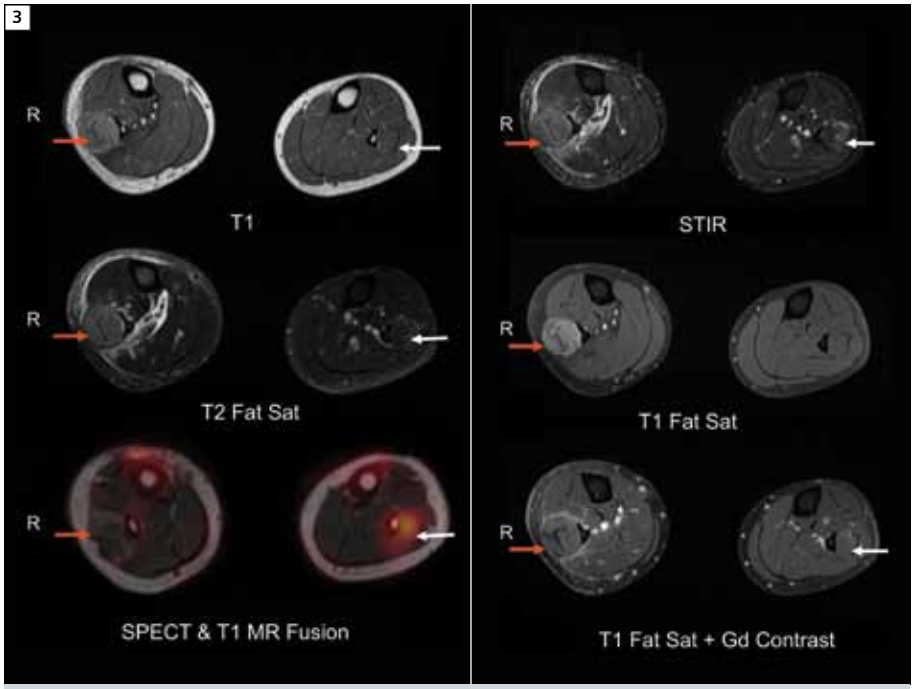

3 Axial MR images and fused SPECT and MR images show the active site of myositis on the left side.

COMMENTS

MRI and SPECT•CT images suggest a bilateral peroneal compartment syndrome secondary to trauma related to the 10 km run, which was part of the daily exercise schedule for the patient. The severe pain on the right side was probably related to peroneal compartment syndrome caused by muscle swelling and hemorrhage and fluid accumulation. The myositis on the left peroneal muscles was associated with comparatively less hemorrhage and lower level of swelling and, consequently, demonstrated increased uptake of ^{99m}Tc MDP, as well as mild hyperintensity on the T2 and STIR images, but the signal intensity was far lower as compared to that of the right side. A muscle biopsy from peroneus longus muscles from both legs demonstrated muscle necrosis, which was attributed to compartment syndrome. The combination of MRI and SPECT•CT was instrumental in characterization of a bilateral muscle lesion, although the symptoms were unilateral. Symbia T advanced reconstruction and highest NEMA sensitivity* allows for small lesions to be reconstructed with more counts in the correct volume, which increases contrast for a better evaluation, as demonstrated in the delineation of left peroneal muscle uptake.

EXAMINATION PROTOCOL

Scanner	*Symbia™ T16*
Dose	***20 mCi ^{99m}Tc MDP***
Parameters	***64 frames, 20 sec /frame***
CT	***130 kV, 40 eff mAs***

* Based on competitive informations available at time of publication. Data on file.

Case 12

SPECT•CT Using ^{99m}Tc MDP and ^{67}Ga for Evaluation of Infection in a Prosthetic Knee Joint

By Ian Duncan, MD

Case study data provided by Bega Valley Radiology, Bega, New South Wales, Australia

HISTORY

A 75-year-old man presented with pain and limited mobility in the prosthetic left knee joint. The patient had a total knee replacement performed 7 years prior. Two years following knee replacement surgery, the patient had an infection in the prosthetic knee joint that was treated conservatively. The patient was free of significant disability following the initial infection until the recent bout of pain and movement restriction in the prosthetic knee joint, which was attributed to a probable infection. There was slight swelling with pain in the knee joint and lower part of the thigh, but without any discharging sinus or skin wound.

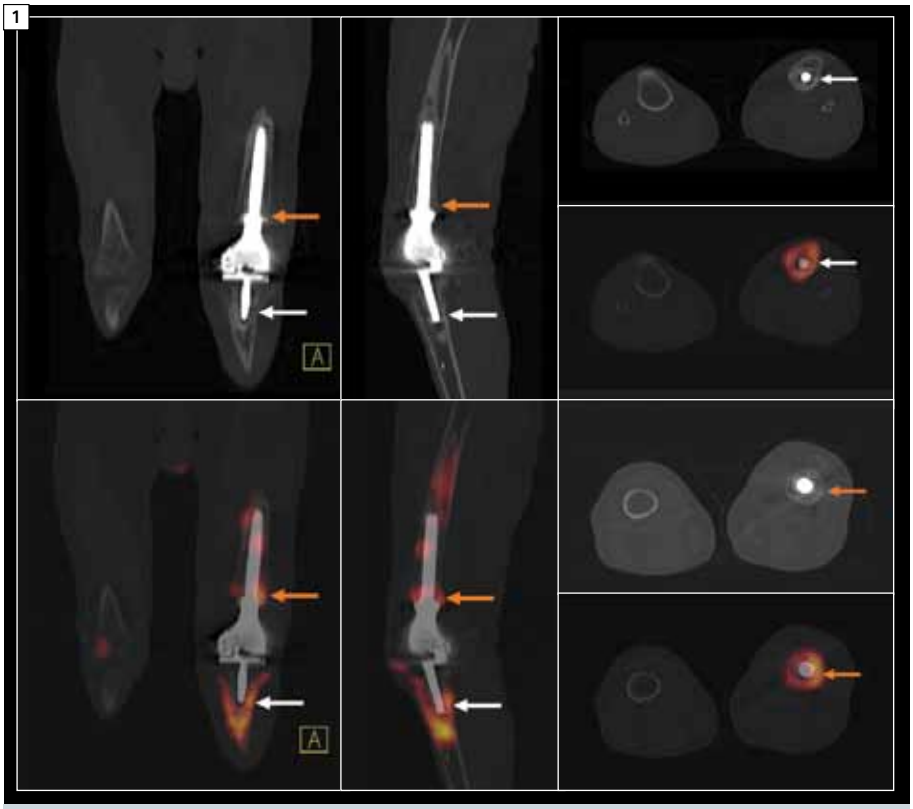

1 ^{99m}Tc MDP study shows periprosthetic bone uptake.

DIAGNOSIS

A technetium-99m methylenediphosphonate (^{99m}Tc MDP) bone SPECT•CT study (*Figure 1*) shows increased skeletal metabolism in the bone around the tibial component of the prosthetic knee joint (*white arrows*), which reflects shear stress secondary to joint movement. Focal increase in uptake at the end of the tibial component may reflect minor loosening of the tibial component as well. CT also shows minor sclerosis around the tibial component. Focal areas of slightly increased uptake of ^{99m}Tc MDP in the bone around the femoral shaft is also related to shear stress due to motion (*red arrows*). The degree of uptake does not reflect any severe increase in bone metabolism (such as osteomyelitis). CT also shows minor sclerosis in the posterior aspect of the bone around the femoral shaft, while the overall density of the cortical bone is reduced compared to the contralateral normal femoral bone.

Since the bone scan was inconclusive for the presence of any joint infection, a gallium-67 (^{67}Ga) SPECT•CT study was performed.

The ^{67}Ga SPECT•CT study (*Figure 2*) shows increased uptake in the lower end of the femoral shaft of the prosthetic knee joint just above the prosthetic condylar component anteriorly with extension of uptake in the soft tissue anterior to the femoral shaft (*red arrows*). Coronal images show extension of ^{67}Ga uptake in the soft tissue

fascial planes upward, suggesting prosthetic joint infection with extension into adjacent soft tissue with upward spread. The femoral condylar part appears uninvolved.
A comparison (*Figure 3*) of ^{67}Ga and ^{99m}Tc MDP bone SPECT and SPECT•CT images at the same imaging plane demonstrates the infective process reflected by gallium uptake in the lower part of the femoral shaft, while bone scintigraphy predominantly shows bone turnover around the lower part of the tibial component of the prosthesis that may reflect minor loosening and movement-related shear stress.

COMMENTS

Absence of significant uptake of gallium, as well as ^{99m}Tc MDP, within the femoral condylar component and the tibial joint surface suggests that the prosthetic joint space was not infected. This suggests that local drainage and debridement of the infected soft tissue in the region of the gallium uptake would be the therapy of choice rather than replacement of the prosthetic joint. Using two separate isotopes, the Symbia™ T6 SPECT•CT with integrated diagnostic CT provided comprehensive information on the true extent of infection and helped make therapy decisions. Symbia T is able to provide the clarity and sharpness required for the visualization of the smallest diagnostic detail as evident in the delineation of the periprosthetic infection.

EXAMINATION PROTOCOL

Scanner	*Symbia T6*
Dose	***20 mCi ^{99m}Tc MDP***
Scan delay	***3 hours post injection***
Parameters	***60 frames, 15 sec/frame***
CT	***130 kV, 40 eff mAs***

Scanner	*Symbia T6*
Dose	***5 mCi ^{67}Ga Citrate***
Scan delay	***24 hours post injection***
Parameters	***64 frames, 30 sec/frame***
CT	***130 kV, 30 eff mAs***

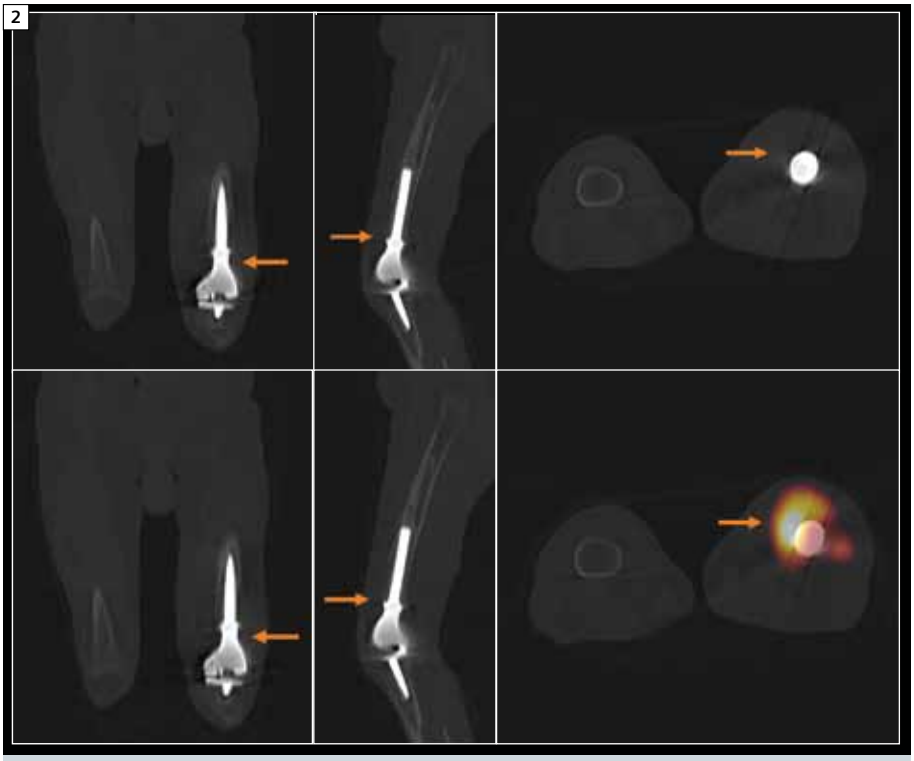

2 ^{67}Ga SPECT•CT shows soft tissue uptake.

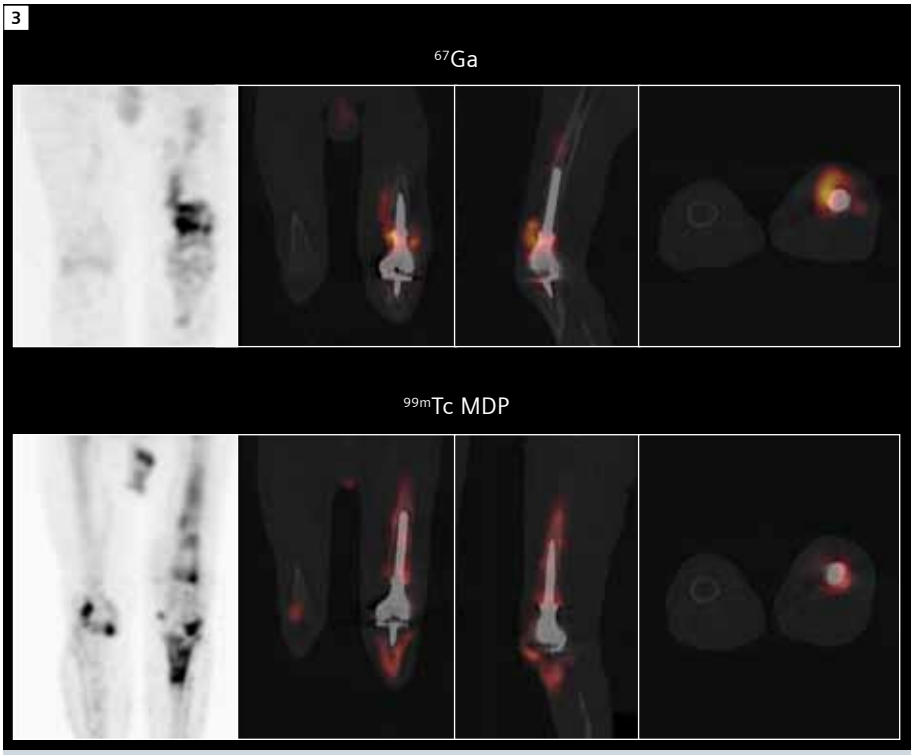

3 Comparison of ^{67}Ga and ^{99m}Tc MDP studies.

Case 13

SPECT•CT-based Characterization of Pseudoarthrosis in Patients with Back Pain Following Lumbar Spinal Fusion

By Olivier Rager, MD

Case study data provided by the University of Geneva, Geneva, Switzerland

INTRODUCTION

Lumbar spinal fusion is commonly performed for spinal instability secondary to degenerative spondylolisthesis, tumor, bone cysts, disc herniation and other causes. Lumbar fusion is often associated with complications such as pseudoarthrosis, which is defined as nonunion even after 6 months following fusion surgery. CT is routinely used to aid the diagnosis of pseudoarthrosis, but may overdiagnose nonunion around the interbody cage. Demonstration of bone resorption around pedicle screws by CT is not always associated with pseudoarthrosis and may lead to false positive predictions. A technetium-99m methylenediphosphonate (^{99m}Tc MDP) bone scan on SPECT•CT with integrated diagnostic CT has been used for improved characterization of pseudoarthrosis following lumbar fusion, as demonstrated in the following cases.

1 An X-ray of the lumbar spine shows pedicular screws in the L4 and L5 vertebrae, as well as the interbody cage. Significant listhesis in the L4-L5 vertebral bodies is also visualized.

CASE 1: HISTORY

A 73-year-old man with a history of degenerative spondylolisthesis, treated with posterior lumbar interbody fusion (PLIF) in L4/L5 vertebrae with bilateral pedicle screws and interbody cages 5 years ago, presented with a recurrence of back pain.

The patient underwent a ^{99m}Tc MDP bone scan using a Symbia™ T6 SPECT•CT scanner with integrated diagnostic CT.

CT showed a pseudoarthrosis with screw loosening involving the right pedicle screw in L4 vertebrae.

Increased uptake of ^{99m}Tc MDP on the fused SPECT•CT image correlates with pedicular screw loosening. A hypodense halo around the right screw of L4 vertebrae seen on CT corresponds to increased skeletal metabolism (*Figure 2, top row*), indicating screw loosening. Increased tracer uptake in the right L3/L4 facet joint (*Figure 2, top row*) reflects degenerative facet arthropathy, which appears normal on CT only.

CT also shows misplacement of the interbody cage at the L4-L5 level, along with listhesis of vertebral bodies and nonunion between L4 and L5. However, there is no corresponding increase in ^{99m}Tc MDP uptake around the interbody cage (*Figure 2, bottom row*). Focal increase in uptake corresponding to the right pedicular screw is visualized in the sagittal fused SPECT•CT slice (*Figure 2, bottom row*).

2 SPECT•CT slices through L4 vertebrae.

3 Post surgery radiography demonstrates additional L3 screw and correction of listhesis between L4 and L5 vertebrae.

DIAGNOSIS

The clear demonstration of loosening of the right screw in L4 vetebrae by the Symbia scan led to treatment by augmented L3/L5 pedicle screw fixation, along with polymethyl methacrylate (PMMA) injection. Since the interbody cages did not show any increased uptake on SPECT despite visible misplacement on CT, they were not replaced because they did not appear to be subject to any shear stress or instability. The demonstration of right L3/L4 facet joint arthropathy on SPECT•CT enhanced by the high SPECT resolution of the Symbia T6 also affected the surgeon's decision to avoid unnecessary interbody cage manipulation.

COMMENTS

Following resurgery and PMMA injection (*Figure 3*), the patient's back pain decreased and he remains symptom-free as per the last follow-up.

EXAMINATION PROTOCOL

Scanner	*Symbia™ T6*
Dose	***20 mCi ^{99m}Tc MDP***
Scan delay	***3 hours post injection***
Parameters	***30 frames, 50 sec/frame***
Matrix	***128x128***
CT	***140 kV, 100 mAs, 2 mm slice***

CASE 2: HISTORY

A 71-year-old man with a history of lumbar spinal surgery (decompressive laminectomy in L2-L4 and L2 vertebroplasty) underwent an operation for lumbar stenosis by posterior transpedicular T12-L4 fixation using fenestrated screws. PMMA was injected into the vertebral bodies through the fenestrated screws for vertebral stabilization. The patient complained of new right lumbar paravertebral pain less than a month following surgery.

4 An X-ray of the lumbar spine shows posterior transpedicular fixation screws from T12 to L4 along with radio-opaque PMMA within the vertebral bodies.

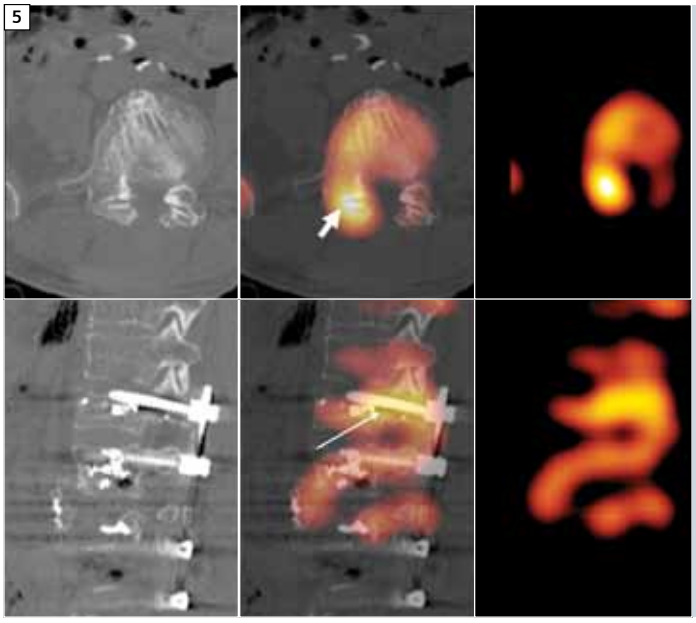

5 SPECT•CT fused images shows intense uptake in the right L4/L5 facet joint (short white arrow, top row), suggesting severe facet arthropathy involving the right facet joint, while the corresponding CT image shows mild symmetrical sclerosis in both facet joints. Intense ^{99m}Tc MDP uptake in this facet joint suggests facet arthropathy as the cause of the new intense lumbar pain.

DIAGNOSIS

Misplacement of the right T12 screw and bone halo around the screw (*thin white arrow, bottom row*) seen on CT, corresponding to the focal area of increased uptake of ^{99m}Tc MDP, is suggestive of a screw loosening with pedicular pseudoarthrosis.
In view of the intense tracer uptake in the L4/L5 right facet joint, the patient received a posterior facet injection of cortisone to treat the articular pain, which led to a dramatic reduction in the pain. Subsequently, the patient underwent an anterior stabilization procedure with L2 corpectomy, insertion of a polyetheretherketone polymer interbody cage (PEEK cage) and stabilization with a lateral plate.
The patient remains symptom-free.

COMMENTS

In this case, the CT-only study was inconclusive for the origin of the pain, since no facet joints demonstrated significant sclerosis. However, the Symbia T6 SPECT•CT study localized the intense uptake of ^{99m}Tc MDP to the right L4/L5 facet joint suggesting severe facet arthropathy, which was treated successfully by intra-articular cortisone injection. This study clearly demostrates the value of Symbia T with integrated CT.

EXAMINATION PROTOCOL

Scanner	*Symbia T6*
Dose	***20 mCi ^{99m}Tc MDP***
Scan delay	***3 hours post injection***
Parameters	***30 frames, 50 sec/frame***
Matrix	***128x128***
CT	***140 kV, 100 mAs, 2 mm slice***

6 A follow-up radiograph of the lumbar spine shows T12 to L4 screws with a lateral stabilization plate.

Case 14
SPECT•CT Using ^{99M}Tc White Blood Cell in Vascular Graft Infection

By Wolfgang Romer, MD

Case study data provided by Klinikum Passau, Passau, Germany

HISTORY

A 70-year-old man presented with a long standing history of peripheral vascular atherosclerotic disease and a 1996 history of placement of polytetrafluoroethylene (PTFE) prosthetic bypass graft connecting femoral artery at the inguinal level to the mid popliteal artery in order to bypass left proximal femoral artery occlusion. The surgery was complicated by development of a peri-prosthetic abscess, which was surgically drained. Patient again presented in November 2011 with pain and swelling in left upper thigh corresponding to the area of previously treated peri-prosthetic abscess. Clinical examination revealed an abscess-like swelling in the medial aspect of the left thigh. The proximal femoral artery at the inguinal level had prominent pulsations, which were felt clinically. Doppler sonography demonstrated slightly lower vascular closing pressures in the lower popliteal and anterior and posterior tibial arteries on the left side as compared to that on the right. Serum markers for inflammation were significantly increased (CRP 158.7 mg/l, with normal range being 0-5 mg/l). In view of the persistently high CRP levels and the clinically apparent abscess in the thigh, an inflammatory process involving the entire vascular prosthesis was suspected. Patient underwent SPECT•CT study after injection of technetium-99m-labeled white blood cells (^{99m}Tc WBC).

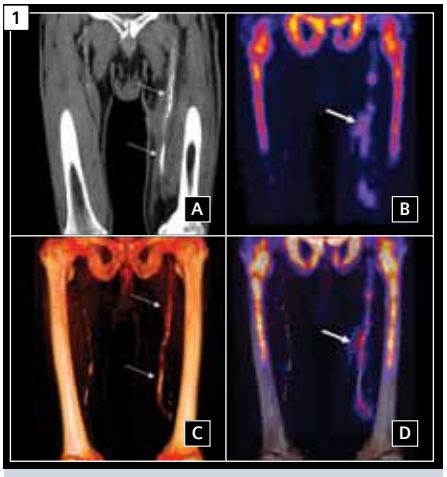

1 Thin MIP (A) and volume rendering (C) of non-contrast enhanced low dose CT show vascular graft (thin white arrows) in the left thigh. MIP image of SPECT study (B) and volume rendering of the fused SPECT•CT data (D) show focal areas of increased uptake of ^{99m}Tc-labeled white blood cells throughout the length of the arterial bypass graft with a collection of tracer in the middle level (thick white arrow), which corresponds to the peri-prosthetic abscess in the medial aspect of the thigh.

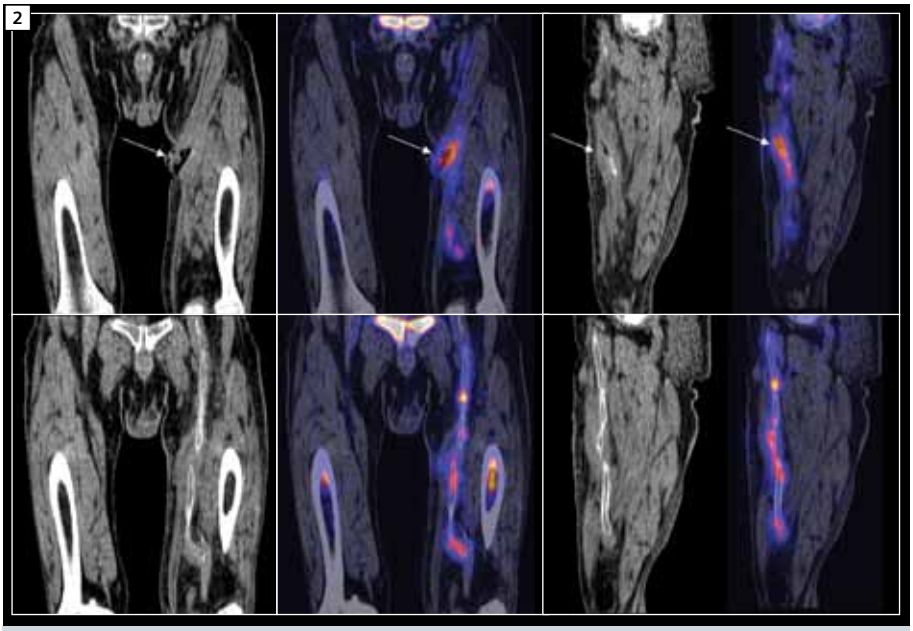

2 Coronal and sagittal slices of CT and fused SPECT•CT images show collection of ^{99m}Tc-labeled white blood cells in the medial aspect of the left thigh (white arrow) corresponding to the abscess adjacent to the femoral vascular prosthetic graft, which also is shown to have an external sinus. The bottom row shows the length of the vascular graft with multiple focal areas of uptake of radiolabeled white blood cells confirming presence of graft infection throughout the entire length of the vascular prosthesis, including the insertion of the lower end of the graft to the popliteal artery.

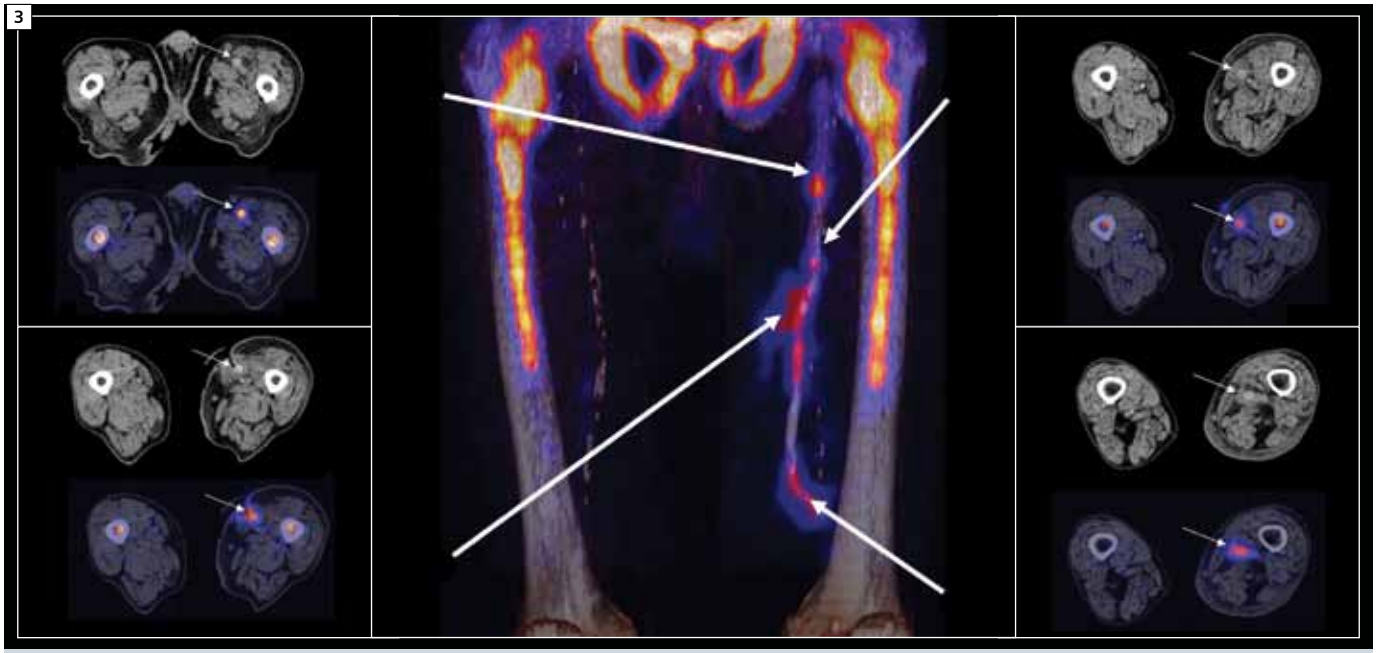

3 Transverse sections at various levels of the femoral graft showing the cross section of the vascular prosthesis and the corresponding increased uptake of radiolabeled white blood cells representing vascular graft infection. Note the tracer uptake beyond the margin of the graft extending into the peri-prosthetic abscess at the level of mid-thigh.

DIAGNOSIS

SPECT•CT with precise fusion of thin-slice integrated diagnostic CT obtained with Symbia™ T6 clearly demonstrates the infection extending throughout the femoral graft with pooling of tracer in the abscess rather than a focal infective foci. High image resolution due to the unique collimator design of Symbia T helps delineate small infective foci within prosthetic graft.*

COMMENTS

The pattern of uptake suggested presence of a peri-prosthetic abscess along with infection of the entire vascular prosthetic graft, which warranted surgery to remove the vascular graft and implant a new bypass graft. A Femoro-Popliteal Goretex bypass was performed along with abscess drainage in December 2011 based on the SPECT•CT findings. Accurate localization of the foci of radiolabeled white blood cells due to integrated low dose CT helped to define the true extent of the infection, as well as the extent of the abscess in the peri-vascular space, which led to the decision of graft removal, new vascular bypass grafting and proper drainage of abscess.

Utilizing Symbia T with low dose CT information for SPECT•CT-based infection imaging provided comprehensive information on the true extent of infection and helped management make therapy decisions, while minimizing the radiation dose to the patient.

EXAMINATION PROTOCOL

Scanner	*Symbia T6*
Dose	***20 mCi ^{99m}Tc WBC***
Scan delay	***5 hours post injection***
Parameters	***64 frames, 30 sec/frame***
CT	***130 kV, 10 eff mAs, 3 mm slice***

* Based on competitive informations available at time of publication. Data on file.

Imaging Life

Publisher:
Siemens Medical Solutions USA, Inc.
Healthcare Sector Molecular Imaging
2501 N. Barrington Road
Hoffman Estates, IL 60192
USA
Telephone: + 1 847 304-7700
www.siemens.com/mi

Editors:
Catherine Eby
kate.eby@siemens.com
Terri McGuire
therese.mcguire@siemens.com

Editorial Assistant: Lauren Caruba

Responsible for Content:
Partha Ghosh, MD

Responsible for Clinical Images:
Patrick Sorger

Design Consulting:
360 Media, Inc., Colorado, USA

Printer: Tewell Warren Printing,
Colorado, USA

HIGHLIGHTS OF PRESCRIBING INFORMATION

These highlights do not include all the information needed to use Fludeoxyglucose F 18 Injection safely and effectively. See full prescribing information for Fludeoxyglucose F 18 Injection.

Fludeoxyglucose F 18 Injection, USP
For intravenous use
Initial U.S. Approval: 2005

RECENT MAJOR CHANGES

Warnings and Precautions	
(5.1, 5.2)	7/2010
Adverse Reactions (6)	7/2010

INDICATIONS AND USAGE

Fludeoxyglucose F18 Injection is indicated for positron emission tomography (PET) imaging in the following settings:

- Oncology: For assessment of abnormal glucose metabolism to assist in the evaluation of malignancy in patients with known or suspected abnormalities found by other testing modalities, or in patients with an existing diagnosis of cancer.
- Cardiology: For the identification of left ventricular myocardium with residual glucose metabolism and reversible loss of systolic function in patients with coronary artery disease and left ventricular dysfunction, when used together with myocardial perfusion imaging.
- Neurology: For the identification of regions of abnormal glucose metabolism associated with foci of epileptic seizures (1).

DOSAGE AND ADMINISTRATION

Fludeoxyglucose F 18 Injection emits radiation. Use procedures to minimize radiation exposure. Screen for blood glucose abnormalities.

- In the oncology and neurology settings, instruct patients to fast for 4 to 6 hours prior to the drug's injection. Consider medical therapy and laboratory testing to assure at least two days of normoglycemia prior to the drug's administration (5.2).
- In the cardiology setting, administration of glucose-containing food or liquids (e.g., 50 to 75 grams) prior to the drug's injection facilitates localization of cardiac ischemia (2.3).

Aseptically withdraw Fludeoxyglucose F 18 Injection from its container and administer by intravenous injection (2).

The recommended dose:

- for adults is 5 to 10 mCi (185 to 370 MBq), in all indicated clinical settings (2.1).
- for pediatric patients is 2.6 mCi in the neurology setting (2.2).

Initiate imaging within 40 minutes following drug injection; acquire static emission images 30 to 100 minutes from time of injection (2).

DOSAGE FORMS AND STRENGTHS

Multi-dose 30mL and 50mL glass vial containing 0.74 to 7.40 GBq/mL (20 to 200 mCi/mL) Fludeoxyglucose
F 18 Injection and 4.5mg of sodium chloride with 0.1 to 0.5% w/w ethanol as a stabilizer (approximately 15 to 50 mL volume) for intravenous administration (3).

CONTRAINDICATIONS

None

WARNINGS AND PRECAUTIONS

- Radiation risks: use smallest dose necessary for imaging (5.1).
- Blood glucose adnormalities: may cause suboptimal imaging (5.2).

ADVERSE REACTIONS

Hypersensitivity reactions have occurred; have emergency resuscitation equipment and personnel immediately available (6).

To report SUSPECTED ADVERSE REACTIONS, contact PETNET Solutions, Inc. at 877-473-8638 or FDA at 1-800-FDA-1088 or www.fda.gov/medwatch.

USE IN SPECIFIC POPULATIONS

Pregnancy Category C: No human or animal data. Consider alternative diagnostics; use only if clearly needed (8.1).

- Nursing mothers: Use alternatives to breast feeding (e.g., stored breast milk or infant formula) for at least 10 half-lives of radioactive decay, if Fludeoxyglucose F 18 Injection is administered to a woman who is breastfeeding (8.3).
- Pediatric Use: Safety and effectiveness in pediatric patients have not been established in the oncology and cardiology settings (8.4).

See 17 for PATIENT COUNSELING INFORMATION

Revised: 1/2011

FULL PRESCRIBING INFORMATION: CONTENTS*

* Sections or subsections omitted from the full prescribing information are not listed.

FULL PRESCRIBING INFORMATION

1 INDICATIONS AND USAGE

Fludeoxyglucose F 18 Injection is indicated for positron emission tomography (PET) imaging in the following settings:

1.1 Oncology

For assessment of abnormal glucose metabolism to assist in the evaluation of malignancy in patients with known or suspected abnormalities found by other testing modalities, or in patients with an existing diagnosis of cancer.

1.2 Cardiology

For the identification of left ventricular myocardium with residual glucose metabolism and reversible loss of systolic function in patients with coronary artery disease and left ventricular dysfunction, when used together with myocardial perfusion imaging.

1.3 Neurology

For the identification of regions of abnormal glucose metabolism associated with foci of epileptic seizures.

2 DOSAGE AND ADMINISTRATION

Fludeoxyglucose F 18 Injection emits radiation. Use procedures to minimize radiation exposure. Calculate the final dose from the end of synthesis (EOS) time using proper radioactive decay factors. Assay the final dose in a properly calibrated dose calibrator before administration to the patient [see Description (11.2)].

2.1 Recommended Dose for Adults

Within the oncology, cardiology and neurology settings, the recommended dose for adults is 5 to 10 mCi (185 to 370 MBq) as an intravenous injection.

2.2 Recommended Dose for Pediatric Patients

Within the neurology setting, the recommended dose for pediatric patients is 2.6 mCi, as an intravenous injection. The optimal dose adjustment on the basis of body size or weight has not been determined [see Use in Special Populations (8.4)].

2.3 Patient Preparation

- To minimize the radiation absorbed dose to the bladder, encourage adequate hydration. Encourage the patient to drink water or other fluids (as tolerated) in the 4 hours before their PET study.
- Encourage the patient to void as soon as the imaging study is completed and as often as possible thereafter for at least one hour.
- Screen patients for clinically significant blood glucose abnormalities by obtaining a history and/or laboratory tests [see Warnings and Precautions (5.2)]. Prior to Fludeoxyglucose F 18 PET imaging in the oncology and neurology settings, instruct patient to fast for 4 to 6 hours prior to the drug's injection.
- In the cardiology setting, administration of glucose-containing food or liquids (e.g., 50 to 75 grams) prior to Fludeoxyglucose F18 Injection facilitates localization of cardiac ischemia

2.4 Radiation Dosimetry

The estimated human absorbed radiation doses (rem/mCi) to a newborn (3.4 kg), 1-year old (9.8 kg), 5-year old (19 kg), 10-year old (32 kg), 15-year old (57 kg), and adult (70 kg) from intravenous administration of Fludeoxyglucose F 18 Injection are shown in Table 1. These estimates were calculated based on human[2] data and using the data published by the International Commission on Radiological Protection[4] for Fludeoxyglucose ^{18} F. The dosimetry data show that there are slight variations in absorbed radiation dose for various organs in each of the age groups. These dissimilarities in absorbed radiation dose are due to developmental age variations (e.g., organ size, location, and overall metabolic rate for each age group). The identified critical organs (in descending order) across all age groups evaluated are the urinary bladder, heart, pancreas, spleen, and lungs.

Table 1. Estimated Absorbed Radiation Doses (rem/mCi) After Intravenous Administration of Fludeoxyglucose F-18 Injection[a]

Organ	Newborn	1-year old	5-year old	10-year old	15-year old	Adult
	(3.4 kg)	(9.8 kg)	(19 kg)	(32 kg)	(57 kg)	(70 kg)
Bladder wall[b]	4.3	1.7	0.93	0.60	0.40	0.32
Heart wall	2.4	1.2	0.70	0.44	0.29	0.22
Pancreas	2.2	0.68	0.33	0.25	0.13	0.096
Spleen	2.2	0.84	0.46	0.29	0.19	0.14
Lungs	0.96	0.38	0.20	0.13	0.092	0.064
Kidneys	0.81	0.34	0.19	0.13	0.089	0.074
Ovaries	0.80	0.8	0.19	0.11	0.058	0.053
Uterus	0.79	0.35	0.19	0.12	0.076	0.062
LLI wall *	0.69	0.28	0.15	0.097	0.060	0.051
Liver	0.69	0.31	0.17	0.11	0.076	0.058
Gallbladder wall	0.69	0.26	0.14	0.093	0.059	0.049
Small intestine	0.68	0.29	0.15	0.096	0.060	0.047
ULI wall **	0.67	0.27	0.15	0.090	0.057	0.046
Stomach wall	0.65	0.27	0.14	0.089	0.057	0.047
Adrenals	0.65	0.28	0.15	0.095	0.061	0.048
Testes	0.64	0.27	0.14	0.085	0.052	0.041
Red marrow	0.62	0.26	0.14	0.089	0.057	0.047
Thymus	0.61	0.26	0.14	0.086	0.056	0.044
Thyroid	0.61	0.26	0.13	0.080	0.049	0.039
Muscle	0.58	0.25	0.13	0.078	0.049	0.039
Bone surface	0.57	0.24	0.12	0.079	0.052	0.041
Breast	0.54	0.22	0.11	0.068	0.043	0.034
Skin	0.49	0.20	0.10	0.060	0.037	0.030
Brain	0.29	0.13	0.09	0.078	0.072	0.070
Other tissues	0.59	0.25	0.13	0.083	0.052	0.042

[a] MIRDOSE 2 software was used to calculate the radiation absorbed dose. Assumptions on the biodistribution based on data from Gallagher et al.1 and Jones et al.2

[b] The dynamic bladder model with a uniform voiding frequency of 1.5 hours was used. *LLI = lower large intestine; **ULI = upper large intestine

2.5 Radiation Safety – Drug Handling

- Use waterproof gloves, effective radiation shielding, and appropriate safety measures when handling Fludeoxyglucose F 18 Injection to avoid unnecessary radiation exposure to the patient, occupational workers, clinical personnel and other persons.
- Radiopharmaceuticals should be used by or under the control of physicians who are qualified by specific training and experience in the safe use and handling of radionuclides, and whose experience and training have been approved by the appropriate governmental agency authorized to license the use of radionuclides.
- Calculate the final dose from the end of synthesis (EOS) time using proper radioactive decay factors. Assay the final dose in a properly calibrated dose calibrator before administration to the patient [see Description (11.2)].
- The dose of Fludeoxyglucose F 18 used in a given patient should be minimized consistent with the objectives of the procedure, and the nature of the radiation detection devices employed.

2.6 Drug Preparation and Administration

- Calculate the necessary volume to administer based on calibration time and dose.
- Aseptically withdraw Fludeoxyglucose F 18 Injection from its container.
- Inspect Fludeoxyglucose F 18 Injection visually for particulate matter and discoloration before administration, whenever solution and container permit.
- Do not administer the drug if it contains particulate matter or discoloration; dispose of these unacceptable or unused preparations in a safe manner, in compliance with applicable regulations.
- Use Fludeoxyglucose F 18 Injection within 12 hours from the EOS.

2.7 Imaging Guidelines

- Initiate imaging within 40 minutes following Fludeoxyglucose F 18 Injection administration.
- Acquire static emission images 30 to 100 minutes from the time of injection.

3 DOSAGE FORMS AND STRENGTHS

Multiple-dose 30 mL and 50 mL glass vial containing 0.74 to 7.40 GBq/mL (20 to 200 mCi/mL) of Fludeoxyglucose F 18 Injection and 4.5 mg of sodium chloride with 0.1 to 0.5% w/w ethanol as a stabilizer (approximately 15 to 50 mL volume) for intravenous administration.

4 CONTRAINDICATIONS

None

5 WARNINGS AND PRECAUTIONS

5.1 Radiation Risks

Radiation-emitting products, including Fludeoxyglucose F 18 Injection, may increase the risk for cancer, especially in pediatric patients. Use the smallest dose necessary for imaging and ensure safe handling to protect the patient and health care worker [see Dosage and Administration (2.5)].

5.2 Blood Glucose Abnormalities

In the oncology and neurology setting, suboptimal imaging may occur in patients with inadequately regulated blood glucose levels. In these patients, consider medical therapy and laboratory testing to assure at least two days of normoglycemia prior to Fludeoxyglucose F 18 Injection administration.

6 ADVERSE REACTIONS

Hypersensitivity reactions with pruritus, edema and rash have been reported in the post-marketing setting. Have emergency resuscitation equipment and personnel immediately available.

7 DRUG INTERACTIONS

The possibility of interactions of Fludeoxyglucose F 18 Injection with other drugs taken by patients undergoing PET imaging has not been studied.

8 USE IN SPECIFIC POPULATIONS

8.1 Pregnancy

Pregnancy Category C

Animal reproduction studies have not been conducted with Fludeoxyglucose F 18 Injection. It is also not known whether Fludeoxyglucose F 18 Injection can cause fetal harm when administered to a pregnant woman or can affect reproduction capacity. Consider alternative diagnostic tests in a pregnant woman; administer Fludeoxyglucose F 18 Injection only if clearly needed.

8.3 Nursing Mothers

It is not known whether Fludeoxyglucose F 18 Injection is excreted in human milk. Consider alternative diagnostic tests in women who are breast-feeding. Use alternatives to breast feeding (e.g., stored breast milk or infant formula) for at least 10 half-lives of radioactive decay, if Fludeoxyglucose F 18 Injection is administered to a woman who is breast-feeding.

8.4 Pediatric Use

The safety and effectiveness of Fludeoxyglucose F 18 Injection in pediatric patients with epilepsy is established on the basis of studies in adult and pediatric patients. In pediatric patients with epilepsy, the recommended dose is 2.6 mCi. The optimal dose adjustment on the basis of body size or weight has not been determined. In the oncology or cardiology settings, the safety and effectiveness of Fludeoxyglucose F 18 Injection have not been established in pediatric patients.

11 DESCRIPTION

11.1 Chemical Characteristics

Fludeoxyglucose F 18 Injection is a positron emitting radiopharmaceutical that is used for diagnostic purposes in conjunction with positron emission tomography (PET) imaging. The active ingredient 2-deoxy-2-[^{18}F]fluoro-D-glucose has the molecular formula of $C_6H_{11}{}^{18}FO_5$ with a molecular weight of 181.26, and has the following chemical structure:

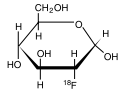

Fludeoxyglucose F 18 Injection is provided as a ready to use sterile, pyrogen free, clear, colorless solution. Each mL contains between 0.740 to 7.40GBq (20.0 to 200 mCi) of 2-deoxy-2-[^{18}F]fluoro-D-glucose at the EOS, 4.5 mg of sodium chloride and 0.1 to 0.5% w/w ethanol as a stabilizer. The pH of the solution is between 4.5 and 7.5. The solution is packaged in a multiple-dose glass vial and does not contain any preservative.

11.2 Physical Characteristics

Fluorine F 18 decays by emitting positron to Oxygen O 16 (stable) and has a physical half-life of 109.7 minutes. The principal photons useful for imaging are the dual 511 keV gamma photons, that are produced and emitted simultaneously in opposite direction when the positron interacts with an electron (Table 2).

Table 2. Pricipal Radiation Emission Data for Fluorine F18

Radiation/Emission	% Per Disintegration	Mean Energy
Positron (b+)	96.73	249.8 keV
Gamma (±)*	193.46	511.0 keV

*Produced by positron annihilation

From: Kocher, D.C. Radioactive Decay Tables DOE/TIC-I 1026, 89 (1981)

The specific gamma ray constant (point source air kerma coefficient) for fluorine F 18 is 5.7 R/hr/mCi (1.35 x 10-6 Gy/hr/kBq) at 1 cm. The half-value layer (HVL) for the 511 keV photons is 4 mm lead (Pb). The range of attenuation coefficients for this radionuclide as a function of lead shield thickness is shown in Table 3. For example, the interposition of an 8 mm thickness of Pb, with a coefficient of attenuation of 0.25, will decrease the external radiation by 75%.

Table 3. Radiation Attenuation of 511 keV Photons by lead (Pb) shielding

Shield thickness (Pb) mm	Coefficient of attenuation
0	0.00
4	0.50
8	0.25
13	0.10
26	0.01
39	0.001
52	0.0001

For use in correcting for physical decay of this radionuclide, the fractions remaining at selected intervals after calibration are shown in Table 4.

Table 4. Physical Decay Chart for Fluorine F18

Minutes	Fraction Remaining
0*	1.000
15	0.909
30	0.826
60	0.683
110	0.500
220	0.250

*calibration time

12 CLINICAL PHARMACOLOGY

12.1 Mechanism of Action

Fludeoxyglucose F 18 is a glucose analog that concentrates in cells that rely upon glucose as an energy source, or in cells whose dependence on glucose increases under pathophysiological conditions. Fludeoxyglucose F 18 is transported through the cell membrane by facilitative glucose transporter proteins and is phosphorylated within the cell to [^{18}F] FDG-6-phosphate by the enzyme hexokinase. Once phosphorylated it cannot exit until it is dephosphorylated by glucose-6-phosphatase. Therefore, within a given tissue or pathophysiological process, the retention and clearance of Fludeoxyglucose F 18 reflect a balance involving glucose transporter, hexokinase and glucose-6-phosphatase activities. When allowance is made for the kinetic differences between glucose and Fludeoxyglucose F 18 transport and phosphorylation (expressed as the ‚lumped constant" ratio), Fludeoxyglucose F 18 is used to assess glucose metabolism.

In comparison to background activity of the specific organ or tissue type, regions of decreased or absent uptake of Fludeoxyglucose F 18 reflect the decrease or absence of glucose metabolism. Regions of increased uptake of Fludeoxyglucose F 18 reflect greater than normal rates of glucose metabolism.

12.2 Pharmacodynamics

Fludeoxyglucose F 18 Injection is rapidly distributed to all organs of the body after intravenous administration. After background clearance of Fludeoxyglucose F 18 Injection, optimal PET imaging is generally achieved between 30 to 40 minutes after administration.

In cancer, the cells are generally characterized by enhanced glucose metabolism partially due to (1) an increase in activity of glucose transporters, (2) an increased rate of phosphorylation activity, (3) a reduction of phosphatase activity or, (4) a dynamic alteration in the balance among all these processes. However, glucose metabolism of cancer as reflected by Fludeoxyglucose F 18 accumulation shows considerable variability. Depending on tumor type, stage, and location, Fludeoxyglucose F 18 accumulation may be increased, normal, or decreased. Also, inflammatory cells can have the same variability of uptake of Fludeoxyglucose F 18.

In the heart, under normal aerobic conditions, the myocardium meets the bulk of its energy requirements by oxidizing free fatty acids. Most of the exogenous glucose taken up by the myocyte is converted into glycogen. However, under ischemic conditions, the oxidation of free fatty acids decreases, exogenous glucose becomes the preferred myocardial sub-

strate, glycolysis is stimulated, and glucose taken up by the myocyte is metabolized immediately instead of being converted into glycogen. Under these conditions, phosphorylated Fludeoxyglucose F 18 accumulates in the myocyte and can be detected with PET imaging.
In the brain, cells normally rely on aerobic metabolism. In epilepsy, the glucose metabolism varies. Generally, during a seizure, glucose metabolism increases. Interictally, the seizure focus tends to be hypometabolic.

12.3 Pharmacokinetics

Distribution: In four healthy male volunteers, receiving an intravenous administration of 30 seconds in duration, the arterial blood level profile for Fludeoxyglucose F 18 decayed triexponentially. The effective half-life ranges of the three phases were 0.2 to 0.3 minutes, 10 to 13 minutes with a mean and standard deviation (STD) of 11.6 (±) 1.1 min, and 80 to 95 minutes with a mean and STD of 88 (±) 4 min.
Plasma protein binding of Fludeoxyglucose F 18 has not been studied.
Metabolism: Fludeoxyglucose F 18 is transported into cells and phosphorylated to [^{18}F]-FDG-6- phosphate at a rate proportional to the rate of glucose utilization within that tissue. [F18]-FDG-6-phosphate presumably is metabolized to 2-deoxy-2-[F18]fluoro-6-phospho-D-mannose([F 18]FDM-6-phosphate).
Fludeoxyglucose F 18 Injection may contain several impurities (e.g., 2-deoxy-2-chloro-D-glucose (ClDG)). Biodistribution and metabolism of ClDG are presumed to be similar to Fludeoxyglucose F 18 and would be expected to result in intracellular formation of 2-deoxy-2-chloro-6-phospho-D-glucose (ClDG-6-phosphate) and 2-deoxy-2-chloro-6-phospho-D-mannose (ClDM-6-phosphate). The phosphorylated deoxyglucose compounds are dephosphorylated and the resulting compounds (FDG, FDM, ClDG, and ClDM) presumably leave cells by passive diffusion. Fludeoxyglucose F 18 and related compounds are cleared from non-cardiac tissues within 3 to 24 hours after administration. Clearance from the cardiac tissue may require more than 96 hours. Fludeoxyglucose F 18 that is not involved in glucose metabolism in any tissue is then excreted in the urine.
Elimination: Fludeoxyglucose F 18 is cleared from most tissues within 24 hours and can be eliminated from the body unchanged in the urine. Three elimination phases have been identified in the reviewed literature. Within 33 minutes, a mean of 3.9% of the administrated radioactive dose was measured in the urine. The amount of radiation exposure of the urinary bladder at two hours post-administration suggests that 20.6% (mean) of the radioactive dose was present in the bladder.
Special Populations:
The pharmacokinetics of Fludeoxyglucose F 18 Injection have not been studied in renally-impaired, hepatically impaired or pediatric patients. Fludeoxyglucose F 18 is eliminated through the renal system. Avoid excessive radiation exposure to this organ system and adjacent tissues.
The effects of fasting, varying blood sugar levels, conditions of glucose intolerance, and diabetes mellitus on Fludeoxyglucose F 18 distribution in humans have not been ascertained [see Warnings and Precautions (5.2)].

13 NONCLINICAL TOXICOLOGY

13.1 Carcinogenesis, Mutagenesis, Impairment of Fertility

Animal studies have not been performed to evaluate the Fludeoxyglucose F 18 Injection carcinogenic potential, mutagenic potential or effects on fertility.

14 CLINICAL STUDIES

14.1 Oncology

The efficacy of Fludeoxyglucose F 18 Injection in positron emission tomography cancer imaging was demonstrated in 16 independent studies. These studies prospectively evaluated the use of Fludeoxyglucose F 18 in patients with suspected or known malignancies, including non-small cell lung cancer, colo-rectal, pancreatic, breast, thyroid, melanoma, Hodgkin's and non-Hodgkin's lymphoma, and various types of metastatic cancers to lung, liver, bone, and axillary nodes. All these studies had at least 50 patients and used pathology as a standard of truth. The Fludeoxyglucose F 18 Injection doses in the studies ranged from 200 MBq to 740 MBq with a median and mean dose of 370 MBq.
In the studies, the diagnostic performance of Fludeoxyglucose F 18 Injection varied with the type of cancer, size of cancer, and other clinical conditions. False negative and false positive scans were observed. Negative Fludeoxyglucose F 18 Injection PET scans do not exclude the diagnosis of cancer. Positive Fludeoxyglucose F 18 Injection PET scans can not replace pathology to establish a diagnosis of cancer. Non-malignant conditions such as fungal infections, inflammatory processes and benign tumors have patterns of increased glucose metabolism that may give rise to false-positive scans. The efficacy of Fludeoxyglucose F 18 Injection PET imaging in cancer screening was not studied.

14.2 Cardiology

The efficacy of Fludeoxyglucose F 18 Injection for cardiac use was demonstrated in ten independent, prospective studies of patients with coronary artery disease and chronic left ventricular systolic dysfunction who were scheduled to undergo coronary revascularization. Before revascularization, patients underwent PET imaging with Fludeoxyglucose F 18 Injection (74 to 370 MBq, 2 to 10 mCi) and perfusion imaging with other diagnostic radiopharmaceuticals. Doses of Fludeoxyglucose F 18 Injection ranged from 74 to 370 MBq (2 to 10 mCi). Segmental, left ventricular, wall-motion assessments of asynergic areas made before revascularization were compared in a blinded manner to assessments made after successful revascularization to identify myocardial segments with functional recovery.
Left ventricular myocardial segments were predicted to have reversible loss of systolic function if they showed Fludeoxyglucose F 18 accumulation and reduced perfusion (i.e., flow-metabolism mismatch). Conversely, myocardial segments were predicted to have irreversible loss of systolic function if they showed reductions in both Fludeoxyglucose F 18 accumulation and perfusion (i.e., matched defects).
Findings of flow-metabolism mismatch in a myocardial segment may suggest that successful revascularization will restore myocardial function in that segment. However, false-positive tests occur regularly, and the decision to have a patient undergo revascularization should not be based on PET findings alone. Similarly, findings of a matched defect in a myocardial segment may suggest that myocardial function will not recover in that segment, even if it is successfully revascularized. However, false-negative tests occur regularly, and the decision to recommend against coronary revascularization, or to recommend a cardiac transplant, should not be based on PET findings alone. The reversibility of segmental dysfunction as predicted with Fludeoxyglucose F 18 PET imaging depends on successful coronary revascularization. Therefore, in patients with a low likelihood of successful revascularization, the diagnostic usefulness of PET imaging with Fludeoxyglucose F 18 Injection is more limited.

14.3 Neurology

In a prospective, open label trial, Fludeoxyglucose F 18 Injection was evaluated in 86 patients with epilepsy. Each patient received a dose of Fludeoxyglucose F 18 Injection in the range of 185 to 370 MBq (5 to 10 mCi). The mean age was 16.4 years (range: 4 months to 58 years; of these, 42 patients were less than 12 years and 16 patients were less than 2 years old). Patients had a known diagnosis of complex partial epilepsy and were under evaluation for surgical treatment of their seizure disorder. Seizure foci had been previously identified on ictal EEGs and sphenoidal EEGs. Fludeoxyglucose F 18 Injection PET imaging confirmed previous diagnostic findings in 16% (14/87) of the patients; in 34% (30/87) of the patients, Fludeoxyglucose F 18 Injection PET images provided new findings. In 32% (27/87), imaging with Fludeoxyglucose F 18 Injection was inconclusive. The impact of these imaging findings on clinical outcomes is not known.
Several other studies comparing imaging with Fludeoxyglucose F 18 Injection results to subsphenoidal EEG, MRI and/or surgical findings supported the concept that the degree of hypometabolism corresponds to areas of confirmed epileptogenic foci. The safety and effectiveness of Fludeoxyglucose F 18 Injection to distinguish idiopathic epileptogenic foci from tumors or other brain lesions that may cause seizures have not been established.

15 REFERENCES

1. Gallagher B.M., Ansari A., Atkins H., Casella V., Christman D.R., Fowler J.S., Ido T., MacGregor R.R., Som P., Wan C.N., Wolf A.P., Kuhl D.E., and Reivich M. "Radiopharmaceuticals XXVII. 18F-labeled 2-deoxy-2-fluoro-d-glucose as a radiopharmaceutical for measuring regional myocardial glucose metabolism in vivo: tissue distribution and imaging studies in animals," J Nucl Med, 1977; 18, 990-6.
2. Jones S.C., Alavi, A., Christman D., Montanez, I., Wolf, A.P., and Reivich M. "The radiation dosimetry of 2 [F-18] fluoro-2-deoxy-D-glucose in man," J Nucl Med, 1982; 23, 613-617.
3. Kocher, D.C. "Radioactive Decay Tables: A handbook of decay data for application to radiation dosimetry and radiological assessments," 1981, DOE/TIC-I 1026, 89.
4. ICRP Publication 53, Volume 18, No. I-4,1987, pages 75-76.

16 HOW SUPPLIED/STORAGE AND DRUG HANDLING

Fludeoxyglucose F 18 Injection is supplied in a multi-dose, capped 30 mL and 50 mL glass vial containing between 0.740 to 7.40 GBq/mL (20 to 200 mCi/mL), of no carrier added 2-deoxy-2-[F 18] fluoro-D-glucose, at end of synthesis, in approximately 15 to 50 mL. The contents of each vial are sterile, pyrogen-free and preservative-free.
NDC 40028-511-30; 40028-511-50
Receipt, transfer, handling, possession, or use of this product is subject to the radioactive material regulations and licensing requirements of the U.S. Nuclear Regulatory Commission, Agreement States or Licensing States as appropriate.
Store the Fludeoxyglucose F 18 Injection vial upright in a lead shielded container at 25°C (77°F); excursions permitted to 15-30°C (59-86°F).
Store and dispose of Fludeoxyglucose F 18 Injection in accordance with the regulations and a general license, or its equivalent, of an Agreement State or a Licensing State.
The expiration date and time are provided on the container label. Use Fludeoxyglucose F 18 Injection within 12 hours from the EOS time.

17 PATIENT COUNSELING INFORMATION

Instruct patients in procedures that increase renal clearance of radioactivity. Encourage patients to:

- drink water or other fluids (as tolerated) in the 4 hours before their PET study.
- void as soon as the imaging study is completed and as often as possible thereafter for at least one hour.

Manufactured by: PETNET Solutions Inc.
810 Innovation Drive
Knoxville, TN 37932

Distributed by: PETNET Solutions Inc.
810 Innovation Drive
Knoxville, TN 37932

PETNET Solutions

PN0002262 Rev. A
March 1, 2011

Global Siemens Headquarters

Siemens AG
Wittelsbacherplatz 2
80333 Muenchen
Germany

Global Siemens Healthcare Headquarters

Siemens AG
Healthcare Sector
Henkestraße 127
91052 Erlangen
Germany
Phone: +49 9131 84 - 0
www.siemens.com/healthcare

www.siemens.com/healthcare-magazine

Order No. A919M1-10336-IC-7600 | Printed in USA | MI-570.KE.360.TW.125 | © 10.2012, Siemens AG

Global Business Unit

Siemens Medical Solutions USA, Inc.
Molecular Imaging
2501 N. Barrington Road
Hoffman Estates, IL 60192
USA
Telephone: + 1 847 304-7700
www.siemens.com/mi

Local Contact Information

Asia/Pacific:
Siemens Medical Solutions
Asia Pacific Headquarters
The Siemens Center
60 MacPherson Road
Singapore 348615
Phone: +65 9622 - 2026
www.siemens.com/healthcare

Canada:
Siemens Canada Limited
Medical Solutions
2185 Derry Road West
Mississauga ON L5N 7A6
Canada
Phone: +1 905 819 - 5800
www.siemens.com/healthcare

Europe/Africa/Middle East:
Siemens AG
Medical Solutions
Henkestraße 127
D-91052 Erlangen
Germany
Phone: +49 9131 84 - 0
www.siemens.com/healthcare

Latin America:
Siemens S.A.
Medical Solutions
Avenida de Pte. Julio A. Roca No 516, Piso 7
C1067ABN Buenos Aires Argentina
Phone: +54 11 4340 - 8400
www.siemens.com/healthcare

USA:
Siemens Medical Solutions USA, Inc.
51 Valley Stream Parkway
Malvern, PA 19355-1406
USA
Phone: +1-888-826 - 9702
www.siemens.com/healthcare